
Jacobian Sparse Autoencoders: Sparsify Computations, Not Just Activations

Lucy Farnik¹ Tim Lawson¹ Conor Houghton¹ Laurence Aitchison¹

Abstract

Sparse autoencoders (SAEs) have been successfully used to discover sparse and human-interpretable representations of the latent activations of LLMs. However, we would ultimately like to understand the computations performed by LLMs and not just their representations. The extent to which SAEs can help us understand computations is unclear because they are not designed to “sparsify” computations in any sense, only latent activations. To solve this, we propose Jacobian SAEs (JSAEs), which yield not only sparsity in the input and output activations of a given model component but also sparsity in the computation (formally, the Jacobian) connecting them. With a naïve implementation, the Jacobians in LLMs would be computationally intractable due to their size. One key technical contribution is thus finding an efficient way of computing Jacobians in this setup. We find that JSAEs extract a relatively large degree of computational sparsity while preserving downstream LLM performance approximately as well as traditional SAEs. We also show that Jacobians are a reasonable proxy for computational sparsity because MLPs are approximately linear when rewritten in the JSAE basis. Lastly, we show that JSAEs achieve a greater degree of computational sparsity on pre-trained LLMs than on the equivalent randomized LLM. This shows that the sparsity of the computational graph appears to be a property that LLMs learn through training, and suggests that JSAEs might be more suitable for understanding learned transformer computations than standard SAEs.

1. Introduction

Sparse autoencoders (SAEs) have emerged as a powerful tool for understanding the internal representations of large language models (Bricken et al., 2023; Cunningham et al., 2023; Gao et al., 2024; Rajamanoharan et al., 2024b;

Lieberum et al., 2024; Lawson et al., 2024; Braun et al., 2024; Kissane et al., 2024; Rajamanoharan et al., 2024a). By decomposing neural network activations into sparse, interpretable components, SAEs have helped researchers gain significant insights into how these models process information (Marks et al., 2024; Lieberum et al., 2024; Templeton et al., 2024b; O’Brien et al., 2024; Farrell et al., 2024; Paulo et al., 2024; Balcells et al., 2024; Lan et al., 2024; Brinkmann et al., 2025; Spies et al., 2024).

When trained on the activation vectors from neural network layers, SAEs learn to reconstruct the inputs using a dictionary of sparse ‘features’, where there are many more features than basis dimensions of the inputs, and each feature tends to capture a specific, interpretable concept. However, the goal of this paper is to improve understanding of *computations* in transformers. While SAEs are designed to disentangle the representations of concepts in the LLM, they are not designed to help us understand the computations performed with those representations. Indeed, SAEs have been shown to exhibit pathological behaviors such as feature absorption, which seem unlikely to be properties of the actual LLM computation (Chanin et al., 2024).

One approach to understanding computation would be to train two SAEs, one at the input and one at the output of an MLP in a transformer. We can then ask how the MLP maps sparse latent features at the inputs to sparse features in the outputs. For this mapping to be interpretable, it would be desirable that it is sparse, in the sense that each latent in the SAE trained on the output depends on a small number of latents of the SAE trained on the input. These dependencies can be understood as a computation graph or ‘circuit’ (Olah et al., 2020; Cammarata et al., 2020). SAEs are not designed to encourage this computation graph to be sparse. To address this, we develop Jacobian SAEs (JSAEs), where we include a term in the objective to encourage SAE bases with sparse computational graphs, not just sparse activations. Specifically, we treat the mapping between the latent activations of the input and output SAEs as a function and encourage its Jacobian to be sparse by including an L^1 penalty term in the loss function.

With a naïve implementation, it is intractable to compute Jacobian matrices because each matrix would have on the order of a trillion elements, even for modestly sized language

¹School of Engineering Mathematics and Technology, University of Bristol, Bristol, UK. Correspondence to: Lucy Farnik <lucyfarnik@gmail.com>.

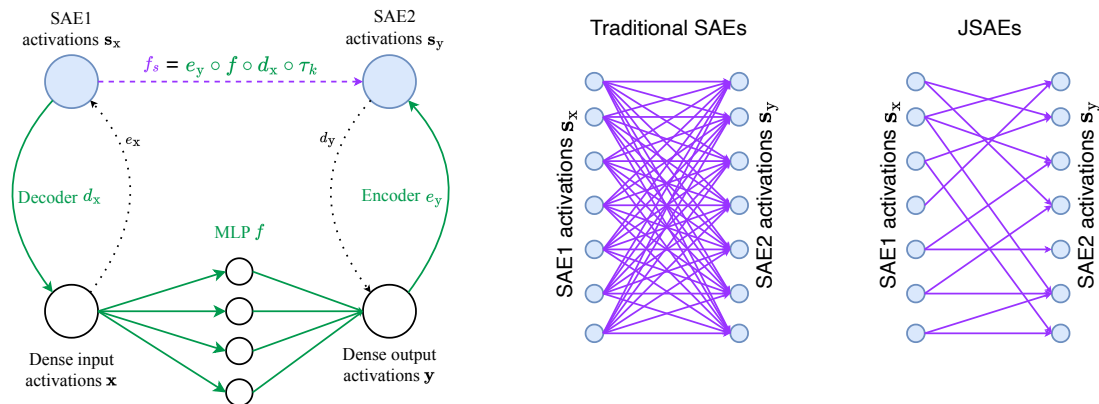


Figure 1. A diagram illustrating our setup. We have two SAEs: one trained on the MLP inputs and the other trained on the MLP outputs. We then consider the function f_s , which takes the latent activations of the first SAE and returns the latent activations of the second SAE, i.e., $f_s(s_x) = s_y$. The function f_s is described by the function composition of the TopK activation function of the first (input) SAE τ_k , the decoder of the first SAE d_x , the MLP f , and the encoder of the second (output) SAE e_y . We note that the activation function τ_k is included for computational efficiency only; see Section 4.2 for details. JSAs optimize for f_s having a sparse Jacobian matrix, which we illustrate by reducing the number of edges in the computational graph that corresponds to f_s . Traditional SAEs have sparse SAE latents on either side of the MLP but a dense computational graph between them; JSAs have both sparse SAE latents *and* a sparse computational graph. Importantly, Jacobian sparsity approximates the computational graph notion, but, as we discuss in Section 5.3 and Appendix B, this approximation is highly accurate due to the fact that f_s is a mostly linear function.

models and SAEs. Therefore, one of our core contributions is to develop an efficient means to compute Jacobian matrices in this context. The approach we develop makes it possible to train a pair of Jacobian SAEs with only approximately double the computational requirements of training a single standard SAE (Section 4.2). These methods enabled us to make three downstream findings.

First, we find that Jacobian SAEs successfully induce sparsity in the Jacobian matrices between input and output SAE latents relative to standard SAEs without a Jacobian term (Section 5.1). We find that JSAs achieve the desired increase in the sparsity of the Jacobian with only a slight decrease in reconstruction quality and model performance preservation, which remain roughly on par with standard SAEs. We also find that the input and output latents learned by Jacobian SAEs are approximately as interpretable as standard SAEs, as quantified by auto-interpretability scores.

Second, inspired by Heap et al. (2025), we investigated the behavior of Jacobian SAEs when applied to random transformers, i.e., where the parameters have been reinitialized. We find that the degree of Jacobian sparsity that can be achieved when JSAs are applied to a pre-trained transformer is much greater than the sparsity achieved for a random transformer (Section 5.2). This preliminary finding suggests that Jacobian sparsity may be a useful tool for discovering learned computational structure.

Lastly, we find that Jacobians accurately approximate computational sparsity in this context because the function we are analyzing (i.e., the combination of JSAs and MLP) is approximately linear (Section 5.3).

Our source code can be found at <https://github.com/lucyfarnik/jacobian-saes>.

2. Related work

2.1. Sparse autoencoders

SAEs have been widely applied to ‘disentangle’ the representations learned by transformer language models into a very large number of concepts, a.k.a. sparse latents, features, or dictionary elements (Sharkey et al., 2022; Cunningham et al., 2023; Bricken et al., 2023; Gao et al., 2024; Rajamanoharan et al., 2024b; Lieberum et al., 2024). Human experiments and quantitative proxies apparently confirm that SAE latents are much more likely to correspond to human-interpretable concepts than raw language-model neurons, i.e., the basis dimensions of their activation vectors (Cunningham et al., 2023; Bricken et al., 2023; Rajamanoharan et al., 2024a). SAEs have been successfully applied to modifying the behavior of LLMs by using a direction discovered by an SAE to “steer” the model towards a certain concept (Makelov, 2024; O’Brien et al., 2024; Templeton et al., 2024b).

Our work is based on SAEs but has a very different aim: standard SAEs only sparsify activations, while JSAEs also sparsify the computation graph between them (Figure 1).

2.2. Transcoders

In this paper, we focus on MLPs. Dunefsky et al. (2024); Templeton et al. (2024a) developed *transcoders*, an alternative SAE-like method to understand MLPs. However, JSAEs and transcoders take radically different approaches and solve radically different problems. This is perhaps easiest to see if we look at what transcoders and JSAEs sparsify. JSAEs are fundamentally an extension of standard SAEs: they train SAEs at the input and output of the MLP and add an extra term to the objective such that these sparse latents are also appropriate for interpreting the MLP (Figure 1). In contrast, transcoders do not sparsify the inputs and outputs; they work with dense inputs and outputs. Instead, transcoders, in essence, sparsify the MLP hidden states. Specifically, a transcoder is an MLP that you train to match (using a mean squared error objective) the input-to-output mapping of the underlying MLP from the transformer. The key difference between the transcoder MLP and the underlying MLP is that the transcoder MLP is much wider, and its hidden layer is trained to be sparse.

Thus, transcoders and JSAEs take fundamentally different approaches. Each transcoder latent tells us ‘there is computation in the MLP related to [concept].’ By comparison, JSAEs learn a pair of SAEs (which have mostly interpretable latents) and sparse connections between them. At a conceptual level, JSAEs tell us that ‘this feature in the MLP’s output was computed using only these few input features’. Ultimately, we believe that the JSAE approach, grounded in understanding how the SAE basis at one layer is mapped to the SAE basis at another layer, is potentially powerful and worth thoroughly exploring.

Importantly, it is worth emphasizing that JSAEs and transcoders are asking fundamentally different questions, as can be seen in terms of e.g., differences in what they sparsify. As such, it is not, to our knowledge, possible to design meaningful quantitative comparisons, at least not without extensive future work to develop very general auto-interpretability methods for evaluating methods of understanding MLP circuits.

2.3. Automated circuit discovery

In “automated circuit discovery”, the goal is to isolate the causally relevant intermediate variables and connections between them necessary for a neural network to perform a given task (Olah et al., 2020). In this context, a circuit is defined as a computational subgraph with an interpretable function. The causal connections between elements are determined via activation patching, i.e., modifying or replacing

the activations at a particular site of the model (Meng et al., 2022; Zhang & Nanda, 2023; Wang et al., 2022; Hanna et al., 2023). In some cases, researchers have identified sub-components of transformer language models with simple algorithmic roles that appear to generalize across models (Olsson et al., 2022).

Conmy et al. (2023) proposed a means to automatically prune the connections between the sub-components of a neural network to the most relevant for a given task using activation patching. Given a choice of task (i.e., a dataset and evaluation metric), this approach to automated circuit discovery (ACDC) returns a minimal computational subgraph needed to implement the task, e.g., previously identified ‘circuits’ like Hanna et al. (2023). Naturally, this is computationally expensive, leading other authors to explore using linear approximations to activation patching (Nanda, 2023; Syed et al., 2024; Kramár et al., 2024). Marks et al. (2024) later improved on this technique by using SAE latents as the nodes in the computational graph.

In a sense, these methods are supervised because they require the user to specify a task. Naturally, it is not feasible to manually iterate over all tasks an LLM can perform, so a fully unsupervised approach is desirable. With JSAEs, we take a step towards resolving this problem, although the architecture introduced in this paper initially only applies to a single MLP layer and not an entire model. Additionally, to the best of our knowledge, no automated circuit discovery algorithm sparsifies the computations inside of MLPs.

3. Background

3.1. Sparse autoencoders

In an SAE, we have input vectors, $\mathbf{x} \in \mathcal{X} = \mathbb{R}^{m_x}$. We want to approximate each vector \mathbf{x} by a sparse linear combination of vectors, $\mathbf{s}_x \in \mathcal{S}_x = \mathbb{R}^{n_x}$. The dimension of the sparse vector, n_x , is typically much larger than the dimension of the input vectors m_x (i.e. the basis is overcomplete).

In the case of SAEs, we treat the vectors as inputs to an autoencoder with an encoder $e_x : \mathcal{X} \rightarrow \mathcal{S}_x$ and a decoder $d_x : \mathcal{S}_x \rightarrow \mathcal{X}$ defined by,

$$\mathbf{s}_x = e_x(\mathbf{x}) = \phi(\mathbf{W}_x^{\text{enc}} \mathbf{x} + \mathbf{b}_x^{\text{enc}}) \quad (1)$$

$$\hat{\mathbf{x}} = d_x(\mathbf{s}_x) = \mathbf{W}_x^{\text{dec}} \mathbf{s}_x + \mathbf{b}_x^{\text{dec}} \quad (2)$$

Here, the parameters are the encoder weights $\mathbf{W}_{\text{enc}} \in \mathbb{R}^{n_x \times m_x}$, decoder weights $\mathbf{W}_{\text{dec}} \in \mathbb{R}^{m_x \times n_x}$, encoder bias $\mathbf{b}_x^{\text{enc}} \in \mathbb{R}^{n_x}$, and decoder bias $\mathbf{b}_x^{\text{dec}} \in \mathbb{R}^{m_x}$. The non-linearity ϕ can be, for instance, ReLU. These parameters are then optimized to minimize the difference between \mathbf{x} and $\hat{\mathbf{x}}$, typically measured in terms of the mean squared error (MSE), while imposing an L^1 penalty on the latent activations \mathbf{s}_x to incentivize sparsity.

3.2. Automatic interpretability of SAE latents

In order to compare the quality of different SAEs, it is desirable to be able to quantify how interpretable its latents are. A popular approach to quantifying interpretability at scale is to collect the examples that maximally activate a given latent, prompt an LLM to generate an explanation of the concept the examples have in common, and then prompt an LLM to predict whether a given prompt activates the SAE latent given the generated explanation. We can then score the accuracy of the predicted activations relative to the ground truth. There are several variants of this approach (e.g., Bills et al., 2023; Choi et al., 2024); in this paper, we use “fuzzing” where the scoring model classifies whether the highlighted tokens in prompts activate an SAE latent given an explanation of that latent (Paulo et al., 2024).

4. Methods

The key idea with a Jacobian SAE is to train a pair of SAEs on the inputs and outputs of a neural network layer while additionally optimizing the sparsity of the Jacobian of the function that relates the input and output SAE latent activations (Figure 1). In this paper, we apply Jacobian SAEs to multi-layer perceptrons (MLPs) of the kind commonly found in transformer language models (Radford et al., 2019; Biderman et al., 2023).

4.1. Setup

Consider an MLP mapping from $\mathbf{x} \in \mathcal{X}$ to $\mathbf{y} \in \mathcal{Y}$, i.e., $f : \mathcal{X} \rightarrow \mathcal{Y}$ or $\mathbf{y} = f(\mathbf{x})$. We can then train two k -sparse SAEs, one on \mathbf{x} and the other on \mathbf{y} . The resulting SAEs map from each of \mathbf{x} and \mathbf{y} to corresponding sparse latents $\mathbf{s}_x \in \mathcal{S}_x$ and $\mathbf{s}_y \in \mathcal{S}_y$, i.e., $\mathbf{s}_x = e_x(\mathbf{x})$ and $\mathbf{s}_y = e_y(\mathbf{y})$, where e_x is the encoder of the first SAE and e_y is the encoder of the second SAE. Each of these SAEs also has a decoder that maps from the sparse latents back to an approximation of the original vector: $\hat{\mathbf{x}} = d_x(\mathbf{s}_x)$ and $\hat{\mathbf{y}} = d_y(\mathbf{s}_y)$.

We may now consider the function $f_s : \mathcal{S}_x \rightarrow \mathcal{S}_y$, which intuitively represents the function, f , but written in terms of the sparse bases learned by the SAE pair for the original vectors \mathbf{x} and \mathbf{y} . Specifically, we define f_s by

$$f_s = e_y \circ f \circ d_x \circ \tau_k \quad (3)$$

where \circ denotes function composition. Here, $d_x : \mathcal{S}_x \rightarrow \mathcal{X}$ maps the sparse latents given as input to f_s to “dense” inputs. Then, $f : \mathcal{X} \rightarrow \mathcal{Y}$ maps the dense inputs to dense outputs. Finally, $e_y : \mathcal{Y} \rightarrow \mathcal{S}_y$ maps the dense outputs to sparse outputs. Note that f_s first applies the TopK activation function τ_k to the sparse inputs, \mathbf{s}_x . Critically, with k -sparse SAEs, we produce the sparse inputs by $\mathbf{s}_x = e_x(\mathbf{x})$, implying that \mathbf{s}_x only has k non-zero elements. In that setting, TopK does not change the inputs, i.e. $\mathbf{s}_x = \tau_k(\mathbf{s}_x)$, but it does affect the

Jacobian and, in particular, allows us to compute it much more efficiently (Section 4.2).

At a high level, we want the function f_s to be ‘sparse’, in the sense that each of its input dimensions (i.e. SAE latent activations) only affects a small number of its output dimensions, and each of its output dimensions only depends on a small number of its input dimensions. We quantify the sparsity of f_s in terms of its Jacobian matrix. The Jacobian of f_s is, in index notation:

$$J_{f_s, i, j} = \frac{\partial f_s(s_{x, i})}{\partial s_{x, j}}. \quad (4)$$

Intuitively, we can consider maximizing the sparsity of the Jacobian as minimizing the number of edges in the computational graph connecting the input and output nodes (Figure 1), i.e. maximizing the number of near-zero elements in the Jacobian matrix. We note that the Jacobian is not a perfect measure of the sparsity of the computational graph, but it is an accurate proxy (see Section 5.3 and Appendix B) while being computationally tractable.

We simultaneously train two separate SAEs on the input and output of a transformer MLP with the objectives of low reconstruction error and sparse relations between the separate SAE latents (via the Jacobian). We do not need to optimize for the sparsity of the latent activations via a penalty term in the loss function because we use k -sparse autoencoders, which keep only the k largest latent activations per token position. Hence, our loss function is

$$\mathcal{L} = \text{MSE}(\mathbf{x}, \hat{\mathbf{x}}) + \text{MSE}(\mathbf{y}, \hat{\mathbf{y}}) + \frac{\lambda}{k^2} \sum_{i=1}^{n_y} \sum_{j=1}^{n_x} |J_{f_s, i, j}| \quad (5)$$

Here, k is the number of non-zero elements in the TopK activation function, n_x, n_y are the dimensionalities of the latent spaces of the input and output SAEs, respectively, and λ is the coefficient of the Jacobian loss term. We divide by k^2 because, as we will see later, there are at most k^2 non-zero elements in the Jacobian. Finally, note that if we set $\lambda = 0$, then our objective effectively trains traditional SAEs for each of \mathbf{x} and \mathbf{y} independently.

4.2. Making the Jacobian calculation tractable

Computing the Jacobian naively (e.g., using an automatic differentiation package) is computationally intractable, as the full Jacobian has size $B \times n_y \times n_x$ where B is the number of tokens in a training batch n_x is the number of SAE latents for the input, and n_y is the number of SAE latents for the output. Unfortunately, typical values are around 1,000 for B and around 32,000 for n_x and n_y (taking as an example a model dimension of 1,000 and an expansion factor of 32). Combined, this gives a Jacobian with around 1 trillion elements. This is obviously far too large to work with in

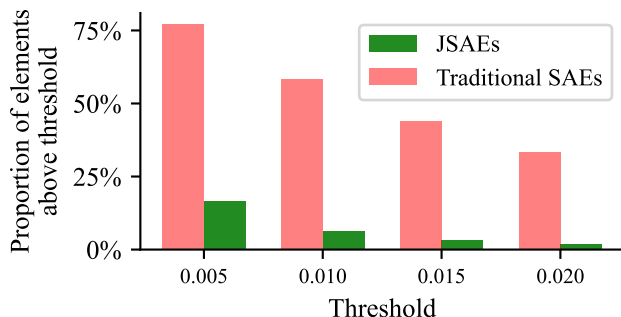


Figure 2. JSAEs induce a much greater degree of sparsity in the elements of the Jacobian of f_s than traditional SAEs. The bars show the average proportion of Jacobian elements with absolute values above certain thresholds. At most $k \times k$ elements can be nonzero, so we take 100% on the y-axis to mean $k \times k$. The average was taken across 10 million tokens. This example is from layer 15 of Pythia-410m. For layer 3 of Pythia-70m and layer 7 of Pythia-160m, see Figure 30, for more quantitative information on Jacobian sparsity across model sizes, layers, and hyperparameters see Figures 20, 21, and 22. We present further discussion of the sparsity of the Jacobian in Appendix E.

practice, and our key technical contribution is to develop an efficient approach to working with this huge Jacobian.

Our first insight is that for each element of the batch, we have a $n_y \times n_x$ Jacobian, where n_x and n_y are around 32,000. This is obviously far too large. However, remember that we are interested in the Jacobian of f_s , so the input is the sparse SAE latent vector, s_x and the output is the sparse SAE latent vector, s_y . Importantly, as we are using k -sparse SAEs, only k elements of the input and output are “on” for any given token. As such, we really only care about the $k \times k$ elements of the Jacobian of f_s , corresponding to the inputs and outputs that are “on”. This reduces the size of the Jacobian by around six orders of magnitude, and renders the computation tractable. However, to make this work formally, we need all elements of the Jacobian corresponding to “off” elements of the input and output to be zero. This is where the τ_k in the definition of f_s becomes important. Specifically, the τ_k ensures that the gradient of f_s wrt any of the inputs that are “off” is zero. Without τ_k , the Jacobian could be non-zero for any of the inputs, even if changing those inputs would not make sense, as it would give more than k elements being “on” in the input, and thus could not be produced by the k -sparse SAE.

Our second insight was that computing the Jacobian by automatic differentiation would still be relatively inefficient, e.g., requiring k backward passes. Instead, for standard GPT-2-style MLPs, we noticed that an extremely efficient Jacobian formula can be derived by hand, requiring only three matrix multiplications and along with a few pointwise

operations. We present this derivation in Appendix A.

With these optimizations in place, training a pair of JSAEs takes about twice as long as training a single standard SAE. We measured this by training ten of each model on Pythia-70m with an expansion factor of 32 for 100 million tokens on an RTX 3090. The average training durations were 72mins for a pair of JSAEs and 33 mins for a traditional SAE, with standard deviations below 30 seconds for both.

5. Results

Our experiments were performed on LLMs from the Pythia suite (Biderman et al., 2023), the figures in the main text contain results from Pythia-410m unless otherwise specified. We trained on 300 million tokens with $k = 32$ and an expansion factor of 64 for Pythia-410m and 32 for smaller models. We reproduced all our experiments on multiple models and found the same qualitative results (see Appendix D).

5.1. Jacobian sparsity, reconstruction quality, and auto-interpretability scores

First, we compared the Jacobian sparsity for standard SAEs and JSAEs. Note that, unlike with SAE latent activations, there is no mechanism for producing exact zeros in the Jacobian elements corresponding to active latents. Hence, we consider the number of near-zero elements rather than the number of exact zeros. To quantify the difference in sparsity between the two, we looked at the proportion of the elements of the Jacobian above a particular threshold when aggregating over 10 million tokens (Figure 2). Here, we found that JSAEs dramatically reduced the number of large elements of the Jacobian relative to traditional SAEs.

Importantly, the degree of sparsity depends on our choice of the coefficient λ of the Jacobian loss term. Therefore, we trained multiple JSAEs with different values of this parameter. As we might expect, for small values of λ , i.e., little incentive to sparsify the Jacobian, the input and output SAEs perform similarly to standard SAEs (Figure 3 blue lines), including in terms of the variance explained by the reconstructed activation vectors and the increase in the cross-entropy loss when the input activations are replaced by their reconstructions. Unsurprisingly, as λ grows larger and the Jacobian loss term starts to dominate, our evaluation metrics degrade. Interestingly, this degradation happens almost entirely in the output SAE rather than the input SAE — we leave it to future work to investigate this phenomenon further.

Critically, Figure 3 suggests there is a ‘sweet spot’ of the λ hyperparameter where the SAE quality metrics remain reasonable, but the Jacobian is much sparser than for standard SAEs. To further investigate this trade-off, we plotted a measure of Jacobian sparsity (the proportion of elements of

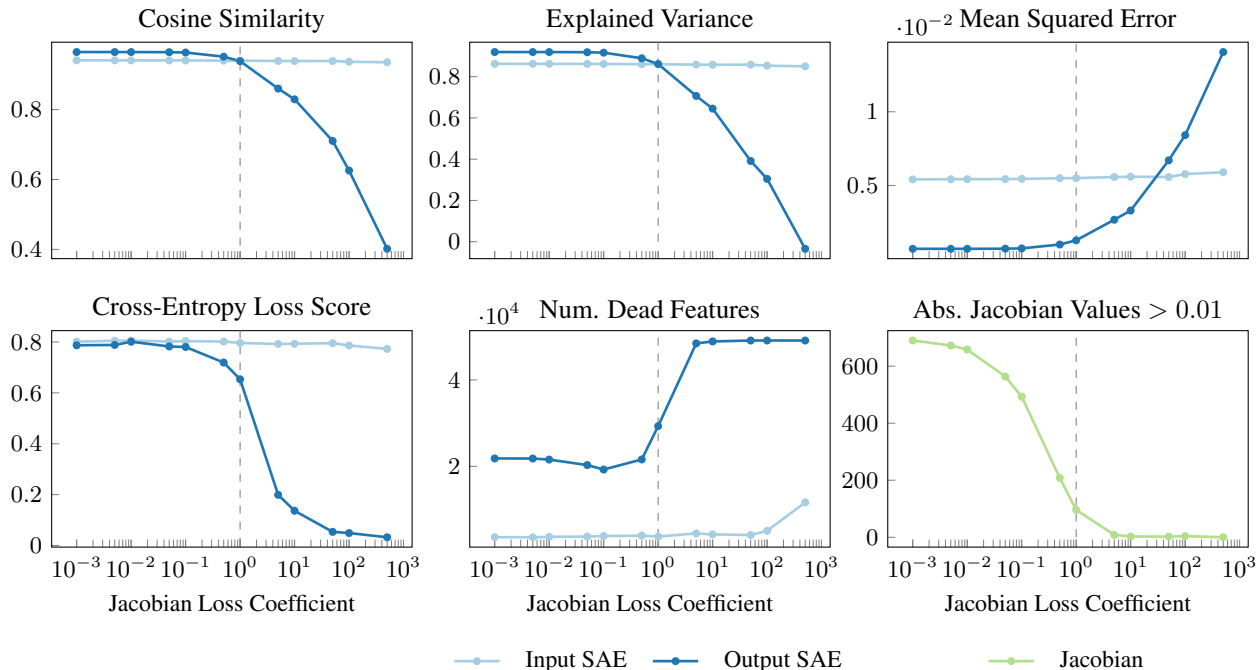


Figure 3. Reconstruction quality, model performance preservation, and sparsity metrics against the Jacobian loss coefficient. JSAEs trained on layer 7 of Pythia-160m with expansion factor 64 and $k = 32$; see Figure 22 for layer 3 of Pythia-70m. Recall that the maximum number of non-zero Jacobian values is $k^2 = 1024$. In accordance with Figure 4, all evaluation metrics degrade for values of the coefficient above 1. See Appendix D for details of the evaluation metrics.

the Jacobian above 0.01) against the average cross-entropy (Figures 3, 4, and 25). We found that there is indeed a sweet spot where the average cross-entropy is only slightly worse than a traditional SAE, while the Jacobian is far sparser. For Pythia 410m (Figure 4) this value is around $\lambda = 0.5$, whereas for Pythia-70m, it is around $\lambda = 1$ (Figure 25). We choose this value of the Jacobian coefficient (i.e. $\lambda = 0.5$ for Pythia-410m in the main text, and $\lambda = 1$ for Pythia-160m in the Appendix) in other experiments.

We also measure the interpretability of JSAE latents using the automatic interpretability pipeline developed by Paulo et al. (2024) and compare this to traditional SAEs. We find that JSAEs achieve similar interpretability scores (Figure 5).

Lastly, we attempted to interpret the pairs of JSAE latents corresponding to the largest Jacobian elements by "max-activating" examples. Though the pairs were generally interpretable, we believe that the problem of interpreting these pairs properly is very subtle and complex (see Appendix F) and leave it to future work to investigate this further.

5.2. Performance on re-initialized transformers

To confirm that JSAEs are extracting information about the complex learned computation, we considered a form of control analysis inspired by Heap et al. (2025). Specifically,

we would expect that trained transformers have carefully learned specific, structured computations while randomly initialized transformers do not. Thus, a possible desideratum for tools in mechanistic interpretability is that they ought to work substantially better when analyzing the complex computations in trained LLMs than when applied to LLMs with randomly re-initialized weights. This is precisely what we find. Specifically, we find that the Jacobians for trained networks are always substantially sparser than the corresponding random trained network, and this holds for both traditional SAEs and JSAEs (Figure 6). Further, the relative improvement in sparsity from the traditional SAE to the JSAE is much larger for trained than random LLMs, again indicating that JSAEs are extracting structure that only exists in the trained network. Note that we also see that for traditional SAEs, there is a somewhat more sparse Jacobian for the trained than randomly initialized transformer. This makes sense: we would hope that the traditional SAE basis is somewhat more aligned with the computation (as expressed by a sparse Jacobian) than we would expect by chance. However, it turns out that without a "helping hand" from the Jacobian sparsity term, the alignment in a traditional SAE is relatively small. Thus, Jacobian sparsity is a property related to the complex computations LLMs learn during training, which should make it substantially useful for discovering the learned structures of LLMs.

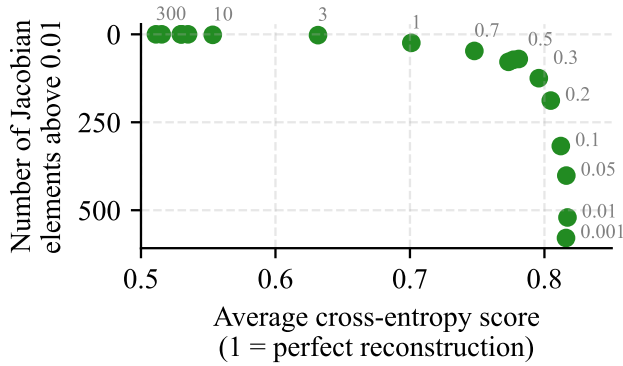


Figure 4. The trade-off between reconstruction quality and Jacobian sparsity as we vary the Jacobian loss coefficient. Each dot represents a pair of JSAs trained with a specific Jacobian coefficient. The value of λ is included for some points. We can see that a coefficient of roughly $\lambda = 0.5$ is optimal for Pythia-410m with $k = 32$. Note that the CE loss score is the average of the CE loss scores of the pre-MLP JSAE and the post-mlp JSAE. Measured on layer 15 of Pythia-410m, similar charts with a wider range of models and metrics can be found in Figures 23, 24, and 25.

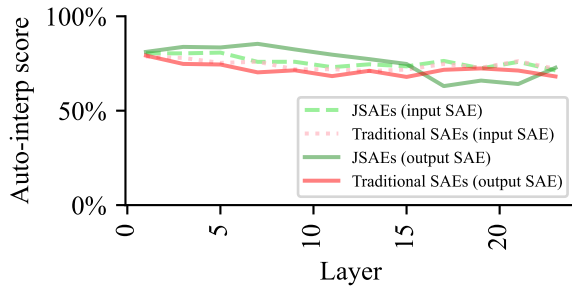


Figure 5. Automatic interpretability scores of JSAs are very similar to traditional SAs. Measured on all odd-numbered layers of Pythia-410m using the “fuzzing” scorer from Paulo et al. (2024). For all layers of Pythia-70m see Figure 32.

5.3. f_s is mostly linear

Importantly, the Jacobian is a local measure. Thus, strictly speaking, a near-zero element of the Jacobian matrix implies only that a small change to the input SAE latent does not affect the corresponding output SAE latent. It may, however, still be the case that a large change to the input SAE latent would change the output SAE latent. We investigated this question and found that f_s is usually approximately linear in a wide range and is often close to linear. Specifically, of the scalar functions relating individual input SAE latents $s_{x,j}$ to individual output SAE latents $s_{y,i}$, the vast majority are linear (Figure 7b). This is important because, for any linear function, its local slope is completely predictive of its global shape, and therefore, a near-zero Jacobian element implies a near-zero causal relationship. For the scalar functions which are not linear, we frequently observed they have a

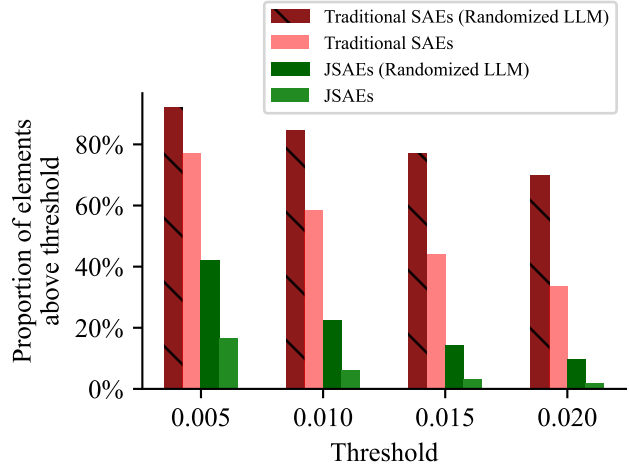


Figure 6. Jacobians are substantially more sparse in pre-trained LLMs than in randomly initialized transformers. This holds both when you actively optimize for Jacobian sparsity with JSAs, and when you don’t optimize for it and use traditional SAs. The figure shows the proportion of Jacobian elements with absolute values above certain thresholds. At most k^2 elements can be nonzero, we therefore take k^2 to be 100% on the y-axis. Jacobians are significantly more sparse in pre-trained transformers than in randomly re-initialized transformers. This shows that Jacobian sparsity is, at least to some extent, connected to the structures that LLMs learn during training. This stands in contrast to recent work by Heap et al. (2025) showing that traditional SAs achieve roughly equal auto-interpretability scores on randomly initialized transformers as they do on pre-trained LLMs. Measured on layer 15 of Pythia-410m, for layer 3 of Pythia-70m see Figure 33. Averaged across 10 million tokens.

JumpReLU structure¹ (Erichson et al., 2019). Notably, a JumpReLU is linear in a subset of its input space, so even for these scalar functions the first derivative is still an accurate measure within some range of $s_{x,j}$ values. It is also worth noting that with JSAs, the proportion of linear functions is noticeably higher than with traditional SAs, so at least to a certain extent, JSAs induce additional linearity in the MLP. To confirm these results, we plotted the Jacobian against the change of output SAE latent $s_{y,i}$ as we change the input SAE latent $s_{x,j}$ by subtracting 1 (Figure 7c)². We found that 97.7% of the time, $|\Delta s_{y,i}| \approx |J_{f_s,ij}|$. For details see Appendix B.

¹By JumpReLU, we mean any function of the form $f(x) = a\text{JumpReLU}(bx + c)$. Recall that $\text{JumpReLU}(x) = x$ if $x > d$ and 0 otherwise. $a, b, c, d \in \mathbb{R}$ are constants.

²For reference, the median value of $s_{x,j}$ without any interventions is 2.5.

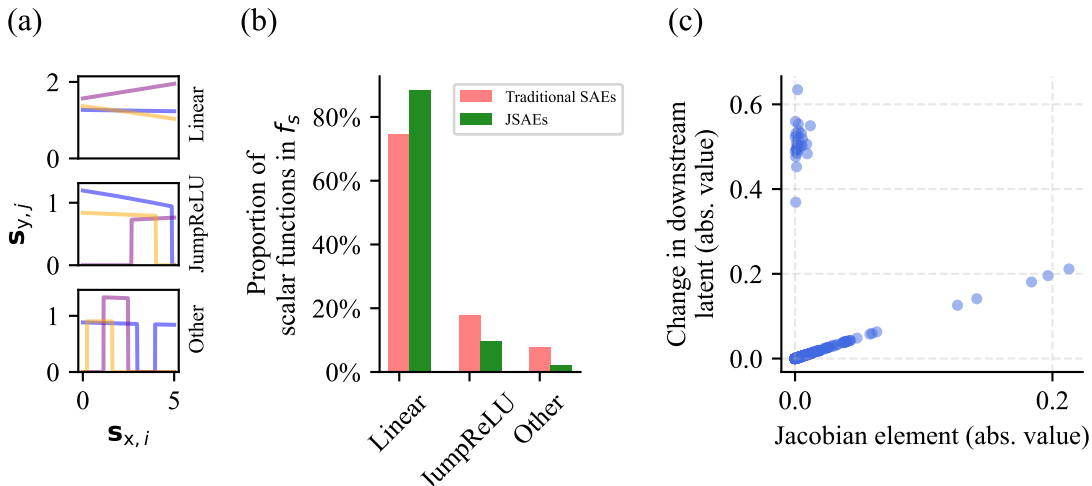


Figure 7. The function f_s , which combines the decoder of the first SAE, the MLP, and the encoder of the second SAE, is mostly linear. Specifically, the vast majority of scalar functions going from $s_{x,j}$ to $s_{y,i}$ are linear. (a) Examples of linear, JumpReLU, and other functions relating individual input SAE latents and output SAE latents. See Figure 8 for more examples. (b) For the empirically observed s_x and randomly selected i, j (of those corresponding to active SAE latents), the vast majority of scalar functions from $s_{x,j}$ to $s_{y,i}$ are linear. For details see Appendix B. The proportion of linear function also noticeably increases with JSAEs compared to traditional SAEs, meaning that JSAEs induce additional linearity in f_s . (c) Because the vast majority of functions are linear, the Jacobian usually precisely predicts the change observed in the output SAE latent when we make a large change to the input SAE latent’s value (namely subtracting 1, note that the empirical median value of $s_{x,j}$ is 2.5). Each dot corresponds to an $(s_{x,j}, s_{y,i})$ pair. For 97.7% of pairs (across a sample size of 10 million) their Jacobian value nearly exactly predicts the change we see in the output SAE latent when making large changes to the input SAE latent’s activation, i.e. $|\Delta s_{y,i}| \approx |J_{f_s, ij}|$. The scatter plot shows a randomly selected subset of 1,000 $(s_{x,j}, s_{y,i})$ pairs. For further details see Appendix B. Measured on layer 15 of Pythia-410m, for layer 3 of Pythia-70m see Figure 34, for the linearity results on other models and hyperparameters see Figures 14, 15, and 16.

6. Discussion

We believe JSAEs are a promising approach for discovering computational sparsity and understanding the reasoning of LLMs. We would also argue that an approach like the one we introduced is in some sense necessary if we want to ‘reverse-engineer’ or ‘decompile’ LLMs into readable source code. It is not enough that our variables (e.g., SAE features) are interpretable; they must also be connected in a relatively sparse way. To illustrate this point, imagine a Python function that takes as input 5 arguments and returns a single variable, and compare this to a Python function that takes 32,000 arguments. Naturally, the latter would be nearly impossible to reason about. Discovering computational sparsity thus appears to be a prerequisite for solving interpretability. It is also important that the mechanisms for discovering computational sparsity be fully unsupervised rather than requiring the user to manually specify the task being analyzed. There are existing methods for taking a specific task and finding the circuit responsible for implementing it, but these require the user to specify the task first (e.g. as a small dataset of task-relevant prompts and a metric of success). They are thus ‘supervised’ in the sense that they need a clear direction from the user. Naturally, it is

not feasible to manually iterate over all tasks an LLM may be performing, so a fully unsupervised approach is needed. JSAEs are the first step in this direction.

Naturally, JSAEs in their current form still have important limitations. They currently only work on MLPs, and for now, they only operate on a single layer at a time rather than discovering circuits throughout the entire model. Our initial implementation also works on GPT-2-style MLPs, while most LLMs from the last few years tend to use GLUs (Dauphin et al., 2017; Shazeer, 2020), though we expect it to be fairly easy to extend our setup to GLUs. Additionally, our current implementation relies on the TopK activation function for efficient batching; TopK SAEs can sometimes encourage high-density features, so it may be desirable to generalize our implementation to work with other activation functions. These are, however, problems that can be addressed relatively straightforwardly in future work, and we would welcome correspondence from researchers interested in addressing them.

A pessimist may argue that partial derivatives (and, therefore, Jacobians) are merely local measures. A small partial derivative tells you that if you slightly tweak the input latent’s activation, you will see no change to the output latent’s

activation, but it may well be the case that a large change to the input latent’s activation will lead to a large change in the output latent. Thankfully, at least in MLPs, this is not quite the case. As we show in Section 5.3, f_s is approximately linear, and the size of the elements of the Jacobian nearly perfectly predicts the change you see in the output latent when you make a large change to the input latent. For a linear function, a first-order derivative at any point is perfectly predictive of the relationship between the input and the output, and thus, at least for the fraction of f_s that is linear, Jacobians perfectly measure the computational relationship between input and output variables. We further discuss this in Appendix B. Additionally, as we showed in Section 5.2, Jacobian sparsity is much more present in trained LLMs than in randomly initialized ones, which indicates that it does correspond in some way to structures that were learned during training. At a high level, a sparse computational graph necessarily implies a sparse Jacobian, but a sparse Jacobian does not in and of itself imply a sparse computational graph. But all of these results make it seem likely that Jacobian sparsity is a good approximation of computational sparsity, and when combined with the fact that we have now developed efficient ways of computing them at scale, this leads us to believe that JSAEs are a highly useful approach. We would, however, still invite future work to further investigate the degree to which Jacobians, and by extension JSAEs, capture the structure we care about when analyzing LLMs.

7. Conclusion

We introduced Jacobian sparse autoencoders (JSAEs), a new approach for discovering sparse computation in LLMs in a fully unsupervised way. We found that JSAEs induce sparsity in the Jacobian matrix of the function that represents an MLP layer in the sparse basis found by JSAEs, with minimal degradation in the reconstruction quality and downstream performance of the underlying model and no degradation in the interpretability of latents. We also found that Jacobian sparsity is substantially greater in pre-trained LLMs than in randomly initialized ones suggesting that Jacobian sparsity is indeed a proxy for learned computational structure. Lastly, we found that Jacobians are a highly accurate measure of computational sparsity due to the fact that the MLP in the JSAE basis consists mostly of linear functions relating input to output JSAE latents.

Acknowledgements

The authors wish to thank Callum McDougall and Euan Ong for helpful discussions. We also thank the contributors to the open-source mechanistic interpretability tooling ecosystem, in particular the authors of SAELens (Bloom et al., 2024), which formed the backbone of our codebase.

The authors wish to acknowledge and thank the financial support of the UK Research and Innovation (UKRI) [Grant ref EP/S022937/1] and the University of Bristol. This work was carried out using the computational facilities of the Advanced Computing Research Centre, University of Bristol - <http://www.bristol.ac.uk/acrc/>. We would like to thank Dr. Stewart for funding for GPU resources.

Impact Statement

The work presented in this paper advances the field of mechanistic interpretability. Our hope is that interpretability will prove beneficial in making LLMs safer and more robust in ways ranging from better detection of model misuse to editing LLMs to remove dangerous capabilities.

Author contribution statement

Conceptualization was done by LF and LA. Derivation of an efficient way to compute the Jacobian was done by LF and LA. Implementation of the training codebase was done by LF. The experiments in Jacobian sparsity, auto-interpretability, reconstruction quality, and approximate linearity of f_s were done by LF. The experiments interpreting feature pairs were done by TL. LA and CH provided supervision and guidance throughout the project. The text was written by LF, LA, TL, and CH. Figures were created by LF and TL with advice from LA and CH.

References

- Balcells, D., Lerner, B., Oesterle, M., Ucar, E., and Heimersheim, S. Evolution of sae features across layers in llms, 2024. URL <https://arxiv.org/abs/2410.08869>.
- Biderman, S., Schoelkopf, H., Anthony, Q. G., Bradley, H., O’Brien, K., Hallahan, E., Khan, M. A., Purohit, S., Prashanth, U. S., Raff, E., Skowron, A., Sutawika, L., and Wal, O. V. D. Pythia: A Suite for Analyzing Large Language Models Across Training and Scaling. In *Proceedings of the 40th International Conference on Machine Learning*, pp. 2397–2430. PMLR, July 2023. URL <https://proceedings.mlr.press/v202/biderman23a.html>.
- Bills, S., Cammarata, N., Mossing, D., Tillman, H., Gao, L., Goh, G., Sutskever, I., Leike, J., Wu, J., and Saunders, W. Language models can explain neurons in language models, May 2023. URL <https://openaipublic.blob.core.windows.net/neuron-explainer/paper/index.html>.
- Bloom, J., Tigges, C., and Chanin, D. SAELens. <https://github.com/jbloomAus/SAELens>, 2024.

- Braun, D., Taylor, J., Goldowsky-Dill, N., and Sharkey, L. Identifying Functionally Important Features with End-to-End Sparse Dictionary Learning, May 2024.
- Bricken, T., Templeton, A., Batson, J., Chen, B., Jermyn, A., Conerly, T., Turner, N., Anil, C., Denison, C., and Askell, A. Towards Monosemanticity: Decomposing Language Models With Dictionary Learning, 2023. URL <https://transformer-circuits.pub/2023/monosemantic-features>.
- Brinkmann, J., Wendler, C., Bartelt, C., and Mueller, A. Large language models share representations of latent grammatical concepts across typologically diverse languages, 2025. URL <https://arxiv.org/abs/2501.06346>.
- Cammarata, N., Carter, S., Goh, G., Olah, C., Petrov, M., Schubert, L., Voss, C., Egan, B., and Lim, S. K. Thread: Circuits. *Distill*, 5(3), March 2020. ISSN 2476-0757. doi: 10.23915/distill.00024.
- Chanin, D., Wilken-Smith, J., Dulka, T., Bhatnagar, H., and Bloom, J. A is for absorption: Studying feature splitting and absorption in sparse autoencoders, 2024. URL <https://arxiv.org/abs/2409.14507>.
- Choi, D., Huang, V., Meng, K., Johnson, D. D., Steinhardt, J., and Schwettmann, S. Scaling Automatic Neuron Description, October 2024. URL <https://transluce.org/neuron-descriptions>.
- Conmy, A., Mavor-Parker, A., Lynch, A., Heimersheim, S., and Garriga-Alonso, A. Towards Automated Circuit Discovery for Mechanistic Interpretability. *Advances in Neural Information Processing Systems*, 36:16318–16352, December 2023.
- Cunningham, H., Ewart, A., Riggs, L., Huben, R., and Sharkey, L. Sparse Autoencoders Find Highly Interpretable Features in Language Models, October 2023.
- Dauphin, Y. N., Fan, A., Auli, M., and Grangier, D. Language modeling with gated convolutional networks, 2017. URL <https://arxiv.org/abs/1612.08083>.
- Dunefsky, J., Chlenski, P., and Nanda, N. Transcoders Find Interpretable LLM Feature Circuits, June 2024.
- Erichson, N. B., Yao, Z., and Mahoney, M. W. Jumprelu: A retrofit defense strategy for adversarial attacks, 2019. URL <https://arxiv.org/abs/1904.03750>.
- Farrell, E., Lau, Y.-T., and Conmy, A. Applying sparse autoencoders to unlearn knowledge in language models, 2024. URL <https://arxiv.org/abs/2410.19278>.
- Gao, L., Biderman, S., Black, S., Golding, L., Hoppe, T., Foster, C., Phang, J., He, H., Thite, A., Nabeshima, N., Presser, S., and Leahy, C. The Pile: An 800GB Dataset of Diverse Text for Language Modeling, December 2020.
- Gao, L., la Tour, T. D., Tillman, H., Goh, G., Troll, R., Radford, A., Sutskever, I., Leike, J., and Wu, J. Scaling and evaluating sparse autoencoders, June 2024.
- Hanna, M., Liu, O., and Variengien, A. How does GPT-2 compute greater-than?: Interpreting mathematical abilities in a pre-trained language model. *Advances in Neural Information Processing Systems*, 36:76033–76060, December 2023.
- Heap, T., Lawson, T., Farnik, L., and Aitchison, L. Sparse autoencoders can interpret randomly initialized transformers, 2025. URL <https://arxiv.org/abs/2501.17727>.
- Kingma, D. P. and Ba, J. Adam: A Method for Stochastic Optimization, January 2017. URL <http://arxiv.org/abs/1412.6980>. arXiv:1412.6980 [cs].
- Kissane, C., Krzyzanowski, R., Bloom, J. I., Conmy, A., and Nanda, N. Interpreting attention layer outputs with sparse autoencoders, 2024. URL <https://arxiv.org/abs/2406.17759>.
- Kramár, J., Lieberum, T., Shah, R., and Nanda, N. Atp*: An efficient and scalable method for localizing llm behaviour to components, 2024. URL <https://arxiv.org/abs/2403.00745>.
- Lan, M., Torr, P., Meek, A., Khakzar, A., Krueger, D., and Barez, F. Sparse autoencoders reveal universal feature spaces across large language models, 2024. URL <https://arxiv.org/abs/2410.06981>.
- Lawson, T., Farnik, L., Houghton, C., and Aitchison, L. Residual Stream Analysis with Multi-Layer SAEs, October 2024.
- Lieberum, T., Rajamanoharan, S., Conmy, A., Smith, L., Sonnerat, N., Varma, V., Kramár, J., Dragan, A., Shah, R., and Nanda, N. Gemma Scope: Open Sparse Autoencoders Everywhere All At Once on Gemma 2, August 2024.
- Makelov, A. Sparse Autoencoders Match Supervised Features for Model Steering on the IOI Task. In *ICML 2024 Workshop on Mechanistic Interpretability*, June 2024. URL <https://openreview.net/forum?id=JdrVuEQih5>.
- Marks, S., Rager, C., Michaud, E. J., Belinkov, Y., Bau, D., and Mueller, A. Sparse Feature Circuits: Discovering and Editing Interpretable Causal Graphs in Language Models, March 2024.

- Meng, K., Bau, D., Andonian, A., and Belinkov, Y. Locating and Editing Factual Associations in GPT. *Advances in Neural Information Processing Systems*, 35:17359–17372, December 2022.
- Nanda, N. Attribution Patching: Activation Patching At Industrial Scale, February 2023. URL <https://www.neelnanda.io/mechanistic-interpretability/attribution-patching>.
- O’Brien, K., Majercak, D., Fernandes, X., Edgar, R., Chen, J., Nori, H., Carignan, D., Horvitz, E., and Poursabzi-Sangde, F. Steering Language Model Refusal with Sparse Autoencoders, November 2024.
- Olah, C., Cammarata, N., Schubert, L., Goh, G., Petrov, M., and Carter, S. Zoom In: An Introduction to Circuits. *Distill*, 5(3), March 2020. ISSN 2476-0757. doi: 10.23915/distill.00024.001.
- Olsson, C., Elhage, N., Nanda, N., Joseph, N., DasSarma, N., Henighan, T., Mann, B., Askell, A., Bai, Y., Chen, A., Conerly, T., Drain, D., Ganguli, D., Hatfield-Dodds, Z., Hernandez, D., Johnston, S., Jones, A., Kernion, J., Lovitt, L., Ndousse, K., Amodei, D., Brown, T., Clark, J., Kaplan, J., McCandlish, S., and Olah, C. In-context Learning and Induction Heads, September 2022.
- Paulo, G., Mallen, A., Juang, C., and Belrose, N. Automatically Interpreting Millions of Features in Large Language Models, October 2024.
- Radford, A., Wu, J., Child, R., Luan, D., Amodei, D., and Sutskever, I. Language Models are Unsupervised Multitask Learners, 2019. URL https://cdn.openai.com/better-language-models/language_models_are_unsupervised_multitask_learners.pdf.
- Raffel, C., Shazeer, N., Roberts, A., Lee, K., Narang, S., Matena, M., Zhou, Y., Li, W., and Liu, P. J. Exploring the limits of transfer learning with a unified text-to-text transformer. *J. Mach. Learn. Res.*, 21(1), January 2020. ISSN 1532-4435.
- Rajamanoharan, S., Conmy, A., Smith, L., Lieberum, T., Varma, V., Kramar, J., Shah, R., and Nanda, N. Improving Sparse Decomposition of Language Model Activations with Gated Sparse Autoencoders. In *ICML 2024 Workshop on Mechanistic Interpretability*, June 2024a. URL <https://openreview.net/forum?id=Ppj5KvzU8Q>.
- Rajamanoharan, S., Lieberum, T., Sonnerat, N., Conmy, A., Varma, V., Kramár, J., and Nanda, N. Jumping Ahead: Improving Reconstruction Fidelity with JumpReLU Sparse Autoencoders, July 2024b. URL <http://arxiv.org/abs/2407.14435>. arXiv:2407.14435 [cs].
- Sharkey, L., Braun, D., and Millidge, B. Taking features out of superposition with sparse autoencoders, December 2022.
- Shazeer, N. Glu variants improve transformer, 2020. URL <https://arxiv.org/abs/2002.05202>.
- Spies, A. F., Edwards, W., Ivanitskiy, M. I., Skapars, A., R auker, T., Inoue, K., Russo, A., and Shanahan, M. Transformers use causal world models in maze-solving tasks, 2024. URL <https://arxiv.org/abs/2412.11867>.
- Syed, A., Rager, C., and Conmy, A. Attribution Patching Outperforms Automated Circuit Discovery. In Belinkov, Y., Kim, N., Jumelet, J., Mohebbi, H., Mueller, A., and Chen, H. (eds.), *Proceedings of the 7th BlackboxNLP Workshop: Analyzing and Interpreting Neural Networks for NLP*, pp. 407–416, Miami, Florida, US, November 2024. Association for Computational Linguistics. doi: 10.18653/v1/2024.blackboxnlp-1.25.
- Templeton, A., Batson, J., Jermyn, A., and Olah, C. Predicting Future Activations, January 2024a. URL <https://transformer-circuits.pub/2024/jan-update/index.html#predict-future>.
- Templeton, A., Conerly, T., Marcus, J., Lindsey, J., Bricken, T., Chen, B., Pearce, A., Citro, C., Ameisen, E., Jones, A., Cunningham, H., Turner, N. L., McDougall, C., MacDiarmid, M., Tamkin, A., Durmus, E., Hume, T., Mosconi, F., Freeman, C. D., Summers, T. R., Rees, E., Batson, J., Jermyn, A., Carter, S., Olah, C., and Henighan, T. Scaling Monosemanticity: Extracting Interpretable Features from Claude 3 Sonnet, May 2024b. URL <https://transformer-circuits.pub/2024/scaling-monosemanticity/index.html>.
- Wang, K., Variengien, A., Conmy, A., Shlegeris, B., and Steinhardt, J. Interpretability in the Wild: a Circuit for Indirect Object Identification in GPT-2 small, November 2022.
- Yun, Z., Chen, Y., Olshausen, B., and LeCun, Y. Transformer visualization via dictionary learning: contextualized embedding as a linear superposition of transformer factors. In Agirre, E., Apidianaki, M., and Vulić, I. (eds.), *Proceedings of Deep Learning Inside Out (DeeLIO): The 2nd Workshop on Knowledge Extraction and Integration for Deep Learning Architectures*, pp. 1–10, Online, June 2021. Association for Computational Linguistics. doi: 10.18653/v1/2021.deelio-1.1.

Zhang, F. and Nanda, N. Towards Best Practices of Activation Patching in Language Models: Metrics and Methods. In *The Twelfth International Conference on Learning Representations*, October 2023. URL <https://openreview.net/forum?id=Hf17y6u9BC>.

A. Efficiently computing the Jacobian

A simple form for the Jacobian of the function $f_s = e_y \circ f \circ d_x \circ \tau_k$, which describes the action of an MLP layer f in the sparse input and output bases, follows from applying the chain rule. Note that here, the subscripts f_s , e_y , etc. denote the function in question rather than vector or matrix indices. For the GPT-2-style MLPs that we study, the components of f_s are:

1. **TopK.** This function takes sparse latents \mathbf{s}_x and outputs sparse latents $\bar{\mathbf{s}}_x$. Importantly, $\mathbf{s}_x = \bar{\mathbf{s}}_x$. This step makes the backward pass of the Jacobian computation more efficient but does not affect the forward pass.

$$\bar{\mathbf{s}}_x = \tau_k(\mathbf{s}_x) \quad (6)$$

2. **Input SAE Decoder.** This function takes sparse latents $\bar{\mathbf{s}}_x$ and outputs dense MLP inputs $\hat{\mathbf{x}}$:

$$\hat{\mathbf{x}} = d_x(\bar{\mathbf{s}}_x) = \mathbf{W}_x^{\text{dec}} \bar{\mathbf{s}}_x + \mathbf{b}_x^{\text{dec}} \quad (7)$$

3. **MLP.** This function takes dense inputs $\hat{\mathbf{x}}$ and outputs dense outputs \mathbf{y} :

$$\mathbf{z} = \mathbf{W}_1 \hat{\mathbf{x}} + \mathbf{b}_1, \quad \mathbf{y} = \mathbf{W}_2 \phi_{\text{MLP}}(\mathbf{z}) + \mathbf{b}_2 \quad (8)$$

where ϕ_{MLP} is the activation function of the MLP (e.g., GeLU in the case of Pythia models).

4. **Output SAE Encoder.** This function takes dense outputs \mathbf{y} and outputs sparse latents \mathbf{s}_y :

$$\mathbf{s}_y = e_y(\mathbf{y}) = \tau_k(\mathbf{W}_y^{\text{enc}} \mathbf{y} + \mathbf{b}_y^{\text{enc}}) \quad (9)$$

The Jacobian $\mathbf{J}_{f_s} \in \mathbb{R}^{n_y \times n_x}$ for a single input activation vector has the following elements, in index notation:

$$J_{f_s,ij} = \frac{\partial s_{y,i}}{\partial s_{x,j}} = \sum_{k\ell mn} \frac{\partial s_{y,i}}{\partial y_k} \frac{\partial y_k}{\partial z_\ell} \frac{\partial z_\ell}{\partial \hat{x}_m} \frac{\partial \hat{x}_m}{\partial \bar{s}_{x,n}} \frac{\partial \bar{s}_{x,n}}{\partial s_{x,j}} \quad (10)$$

We compute each term like so:

1. **Output SAE Encoder derivative:**

$$\frac{\partial s_{y,i}}{\partial y_k} = \tau_k' \left(\sum_j W_{ij}^{\text{enc}} y_j + b_{\text{enc},i} \right) W_{y,ik}^{\text{enc}} = \begin{cases} W_{y,ik}^{\text{enc}} & \text{if } i \in \mathcal{K}_2 \\ 0 & \text{otherwise} \end{cases} \quad (11)$$

where \mathcal{K}_2 is the set of indices selected by the TopK activation function τ_k of the second (output) SAE. Importantly, the subscript k *does not* indicate the k -th element of τ_k , whereas it *does* indicate the k -th column of $W_{y,ik}^{\text{enc}}$.

2. **MLP derivatives:**

$$\frac{\partial y_k}{\partial z_\ell} = W_{2,k\ell} \phi'_{\text{MLP}}(z_\ell), \quad \frac{\partial z_\ell}{\partial \hat{x}_m} = W_{1,\ell m} \quad (12)$$

3. **Input SAE Decoder derivative:**

$$\frac{\partial \hat{x}_m}{\partial \bar{s}_{x,n}} = W_{x,mn}^{\text{dec}} \quad (13)$$

4. **TopK derivative:**

$$\frac{\partial \bar{s}_{x,n}}{\partial s_{x,j}} = \begin{cases} 1 & \text{if } j \in \mathcal{K}_1 \\ 0 & \text{otherwise} \end{cases} \quad (14)$$

where \mathcal{K}_1 is the set of indices (corresponding to SAE latents) that were selected by the TopK activation function τ_k of the first (input) SAE, which we explicitly included in the definition of f_s above.

When we combine all the terms:

$$J_{f_s, ij} = \begin{cases} \sum_{k\ell m} W_{y, ik}^{\text{enc}} W_{2, k\ell} \phi'_{\text{MLP}}(z_\ell) W_{1, \ell m} W_{x, mj}^{\text{dec}} & \text{if } i \in \mathcal{K}_2 \wedge j \in \mathcal{K}_1 \\ 0 & \text{otherwise} \end{cases} \quad (15)$$

Let $\mathbf{W}_y^{\text{enc(active)}} \in \mathbb{R}^{k \times m_y}$ and $\mathbf{W}_x^{\text{dec(active)}} \in \mathbb{R}^{m_x \times k}$ contain the active rows and columns, i.e., the rows and columns corresponding to the \mathcal{K}_2 or \mathcal{K}_1 indices respectively. The Jacobian then simplifies to:

$$\mathbf{J}_{f_s}^{\text{(active)}} = \underbrace{\mathbf{W}_y^{\text{enc(active)}} \mathbf{W}_2}_{\mathbb{R}^{k \times d_{\text{MLP}}}} \cdot \underbrace{\phi'_{\text{MLP}}(\mathbf{z})}_{\mathbb{R}^{d_{\text{MLP}} \times d_{\text{MLP}}}} \cdot \underbrace{\mathbf{W}_1 \mathbf{W}_x^{\text{dec(active)}}}_{\mathbb{R}^{d_{\text{MLP}} \times k}} \quad (16)$$

where d_{MLP} is the hidden size of the MLP. Note that $\mathbf{J}_{f_s}^{\text{(active)}}$ is of size $k \times k$, while the full Jacobian matrix \mathbf{J}_{f_s} is of size $n_y \times n_x$. However, $\mathbf{J}_{f_s}^{\text{(active)}}$ contains all the nonzero elements of \mathbf{J}_{f_s} , so it is all we need to compute the loss function to train Jacobian SAEs (Section 4.1).

B. f_s is approximately linear

Consider the scalar function $f_{s, (i,j)}|_{\mathbf{s}_x} : \mathbb{R} \rightarrow \mathbb{R}$ which takes as input the j -th latent activation of the first SAE (i.e. $s_{x,j}$) and returns as output the i -th latent activation of the second SAE (i.e., $s_{y,i}$), while keeping the other elements of the input vector fixed at the same values as \mathbf{s}_x . In other words, this function captures the relationship between the j -th input SAE latent and the i -th output SAE latent in the context of \mathbf{s}_x . Geometrically, we start off at the point \mathbf{s}_x , and we move from it through the input spaces in parallel to the j -th basis vector, and then we observe how the output of f_s projects onto the i -th basis vector. Formally,

$$f_{s, (i,j)}|_{\mathbf{s}_x}(x) = f_s(\psi(\mathbf{s}_x, i, x))_j \quad (17)$$

$$\psi(\mathbf{s}_x, i, x)_k = \begin{cases} x & \text{if } i = k \\ s_{x,j} & \text{otherwise} \end{cases} \quad (18)$$

These are the functions shown in Figure 7a, of which the vast majority are linear (Figure 7b).

As we showed in Figure 7c, the absolute value of a Jacobian element nearly perfectly predicts the change we see in the output SAE latent activation value when we make a large intervention on the input SAE latent activation. However, in the same figure, there is a small cluster of approximately 2.5% of samples, where the Jacobian element is near zero, but the change observed in the downstream feature is quite large. We proceed by exploring the cause behind this phenomenon.

Note that each point in Figure 7 corresponds to a single scalar function $f_{s, (i,j)}|_{\mathbf{s}_x}$ (a pair of latent indices). An expanded version of Figure 7 is presented in Figure 9. Importantly, we show the ‘line’, the top-left cluster, and outliers visible in Figure 7 in different colors, which we re-use in the following charts (Figures 10 and 11). It also includes 10K samples, compared to 1K in Figure 7c: as above, most samples remain on the line, but the greater number of samples makes the behavior of the top-left cluster and outliers clearer.

Figure 10 illustrates some examples of functions $f_{s, (i,j)}|_{\mathbf{s}_x}$ taken from each category shown in Figure 7, i.e., the line, cluster, and outliers. The vast majority of functions belong to the line category and are typically either linear or akin to JumpReLU activation functions (which include step functions as a special case). By contrast, the minority of functions belonging to the cluster or outliers are typically also JumpReLU-like, except where the unmodified input latent activation is close to the point where the function ‘jumps’, so when we subtract an activation value of 1 from the input (as in Figures 7c and 9), this moves to the flat region where the output latent activation value is zero.

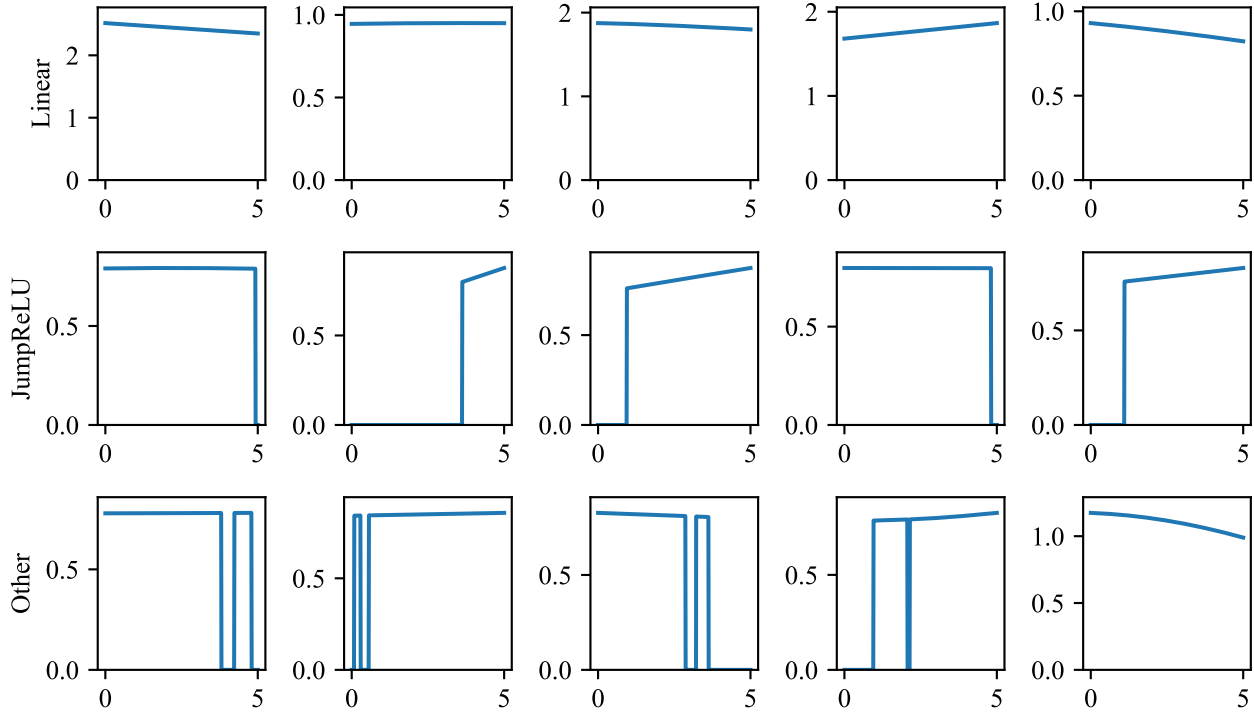


Figure 8. Additional examples of scalar functions between $s_{x,j}$ to $s_{y,i}$. The top row shows linear functions, the middle row shows JumpReLU functions, and the bottom row shows other functions. Recall that linear functions constitute a majority of the functions we observe empirically and that using JSAEs instead of traditional SAEs further increases the proportion of linear functions.

As we can see, the vast majority of these functions are either linear or JumpReLUs. Indeed, we verify this across the sample size of 10,000 functions and find that 88% are linear, 10% are JumpReLU (excl. linear, which is arguably a special case of JumpReLU), and only 2% are neither³. This result is encouraging – for a linear function, the first-order derivative is constant, so its value (i.e., the corresponding element of the Jacobian) completely expresses the relationship between the input and output values (up to a constant intercept). For the 88% of these scalar functions that are linear, the Jacobian thus accurately captures the notion of computational sparsity that interests us, rather than serving only as a proxy. And for the 10% of JumpReLUs, the Jacobians still perfectly measure the computational change we observe when changing the input latent within some subset of the input space.

While we expect the remaining 2% of scalar functions (Jacobian elements) to contribute only a small fraction of the computational structure of the underlying model, we preliminarily investigated their behavior. Figure 11 shows 12 randomly selected non-linear, non-JumpReLU $f_{s,(i,j)}|_{s_x}$ functions. Even though these functions are nonlinear, they are still reasonably close to being linear, i.e., their first derivative is still predictive of the change we see throughout the input space. Indeed, most of them are on the diagonal line in Figure 9.

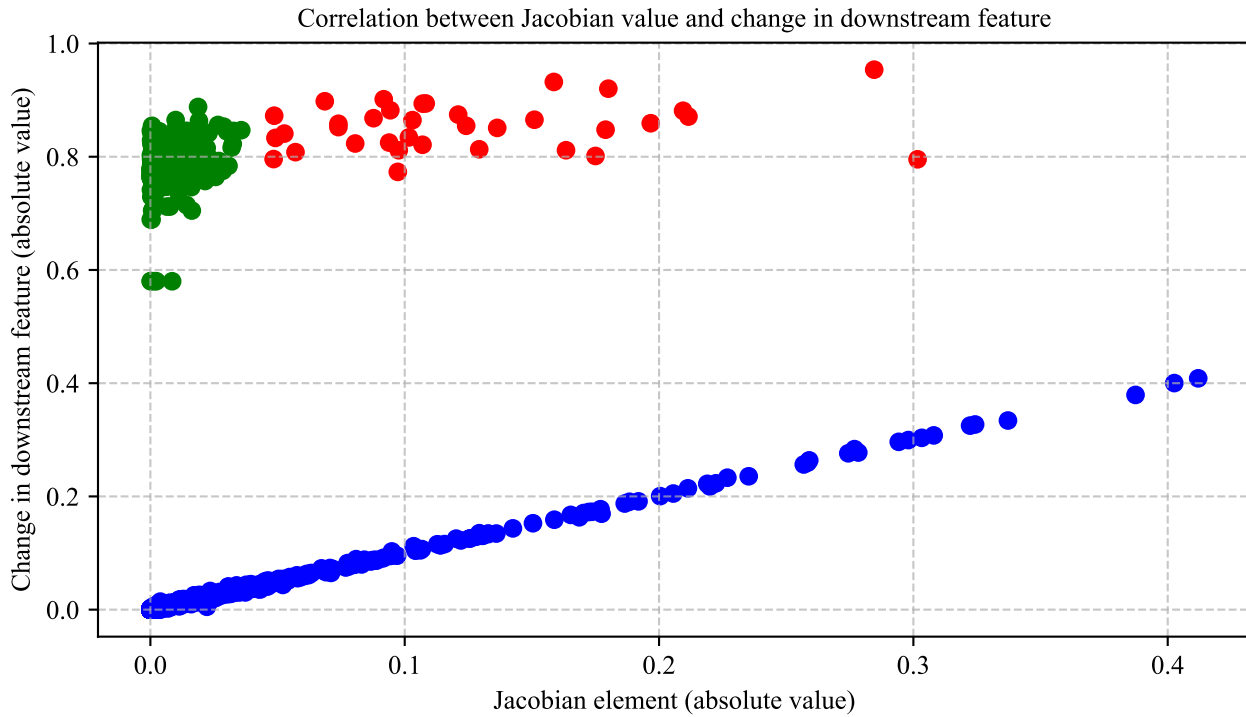


Figure 9. An expanded version of Figure 7c, measured on layer 3 of Pythia-70m. A scatter plot showing that values of Jacobian elements tend to be approximately equal to the change we see in the downstream feature when we modify the value of the upstream feature, namely when we subtract 1 from it. Each dot corresponds to an (input SAE latent, output SAE latent) pair. Unlike Figure 7c, this figure colors in the dots depending on which cluster they belong to – blue for "on the line", green for "in the cluster", red for "outlier". Additionally, this figure contains 10,000 samples (rather than 1,000 as in Figure 7c), which allows us to see more of the outliers and edge cases, though at the cost of visually obfuscating the fact that 97.5% of the samples are on the diagonal line, 2.1% are in the cluster, and 0.4% are outliers.

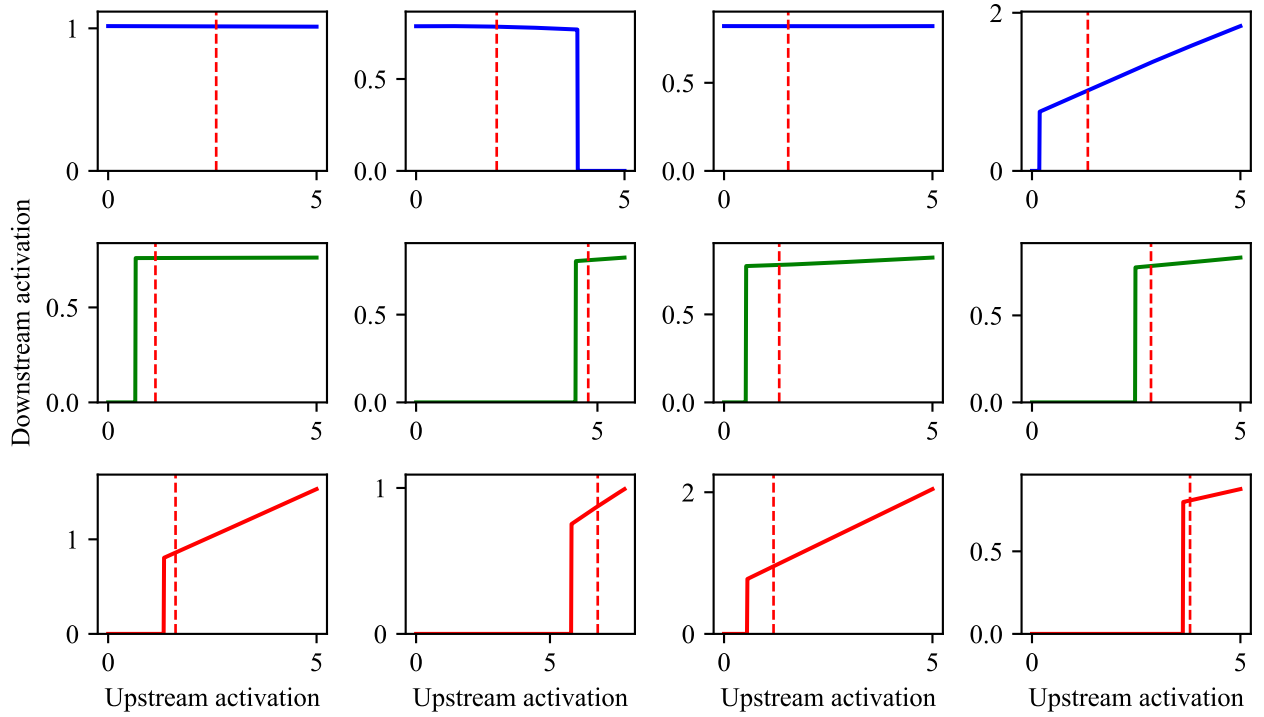


Figure 10. A handful of $f_{s,(i,j)|s_x}$ functions corresponding to the points in Figure 9. The color matches the group (and therefore the color) they were assigned in Figure 9. The red dashed vertical line denotes $s_{x,i}^{(l)}$, i.e. the activation value of the SAE latent before we intervened on it. Note that the functions are not selected randomly but rather hand-selected to demonstrate the range of functions. We will quantitatively explore what proportion of $f_{s,(i,j)|s_x}$ functions have which structure in other figures.

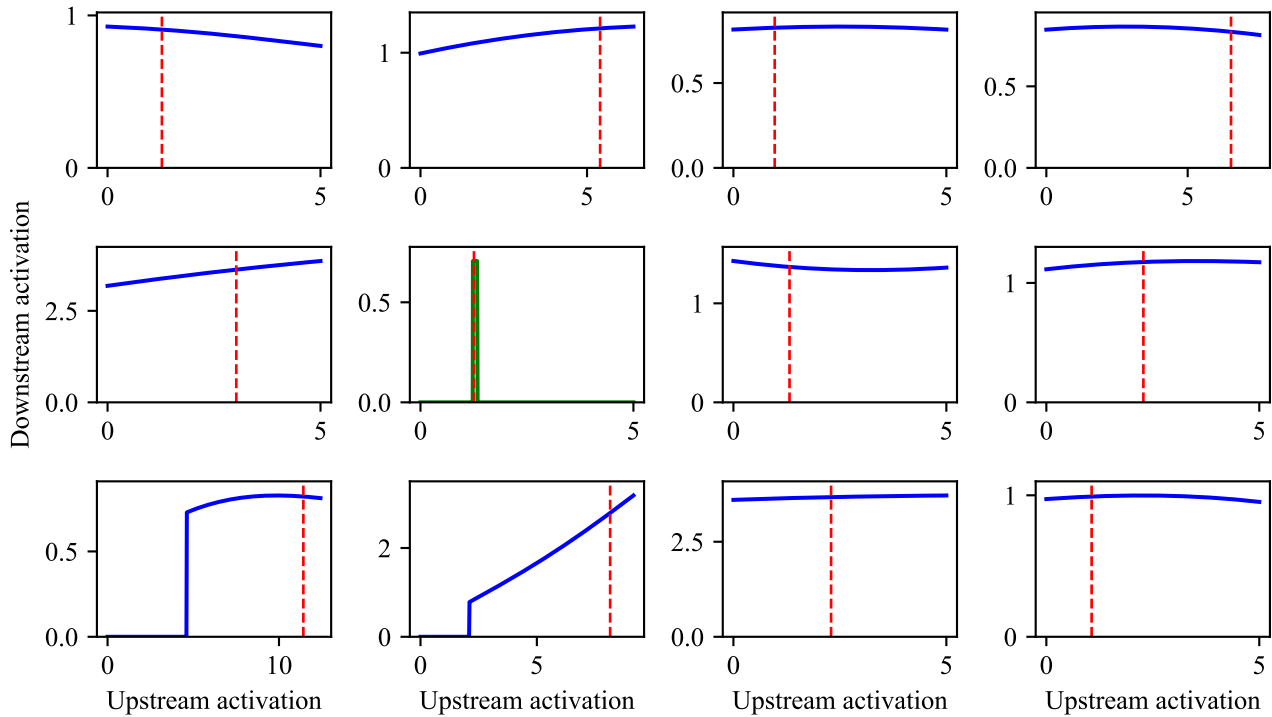


Figure 11. A random selection of the non-linear, non-JumpReLU $f_{s,(i,j)|s_x}$ functions. Note that non-linear, non-JumpReLU functions only constitute about 2% of $f_{s,(i,j)|s_x}$ functions. Even though these functions are clearly somewhat non-linear, their slope does still change quite slowly for the most part, which means that a first-order derivative at any point in the function is still reasonably predictive of the function’s behavior in at least some portion of the input space (though there are some rare exceptions). The color again matches the group (and therefore the color) they were assigned in Figure 9; the red dashed vertical line denotes $s_{x,i}^{(l)}$, i.e. the activation value of the SAE latent before we intervened on it.

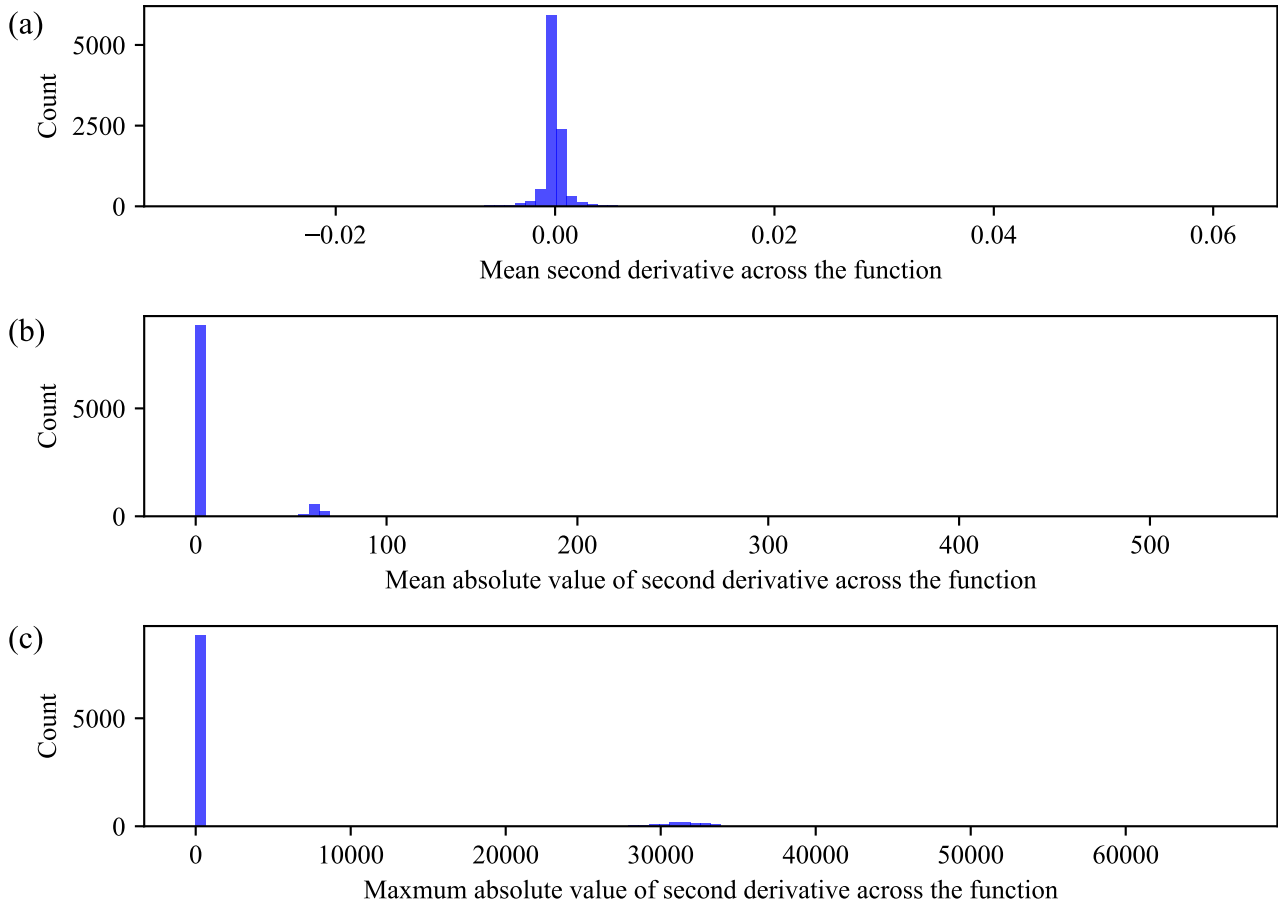


Figure 12. Distribution of second-order derivatives of functions $f_{s,(i,j)}|_{s_x}$. Includes all functions, regardless of whether they are linear, JumpReLU, or neither. For a version that only includes non-linear, non-JumpReLU functions, see Figure 13. (a) The mean of the second-order derivative over the region of the input space. (b) The mean of the absolute value of the second-order derivative over the region of the input space. (c) The maximum value the second-order derivative takes in the region of the input space. Note that we are approximating the second derivative by looking at changes over a very small region (specifically 0.005), i.e., we do not take the limit as the size of this small region goes to zero; this is important because derivatives which would otherwise be undefined or infinite become finite with this approximation and therefore can be shown on the histograms. Also, we note that the means and maxima are taken over the region of the input space in which SAE features exist; see the footnote on page 15.

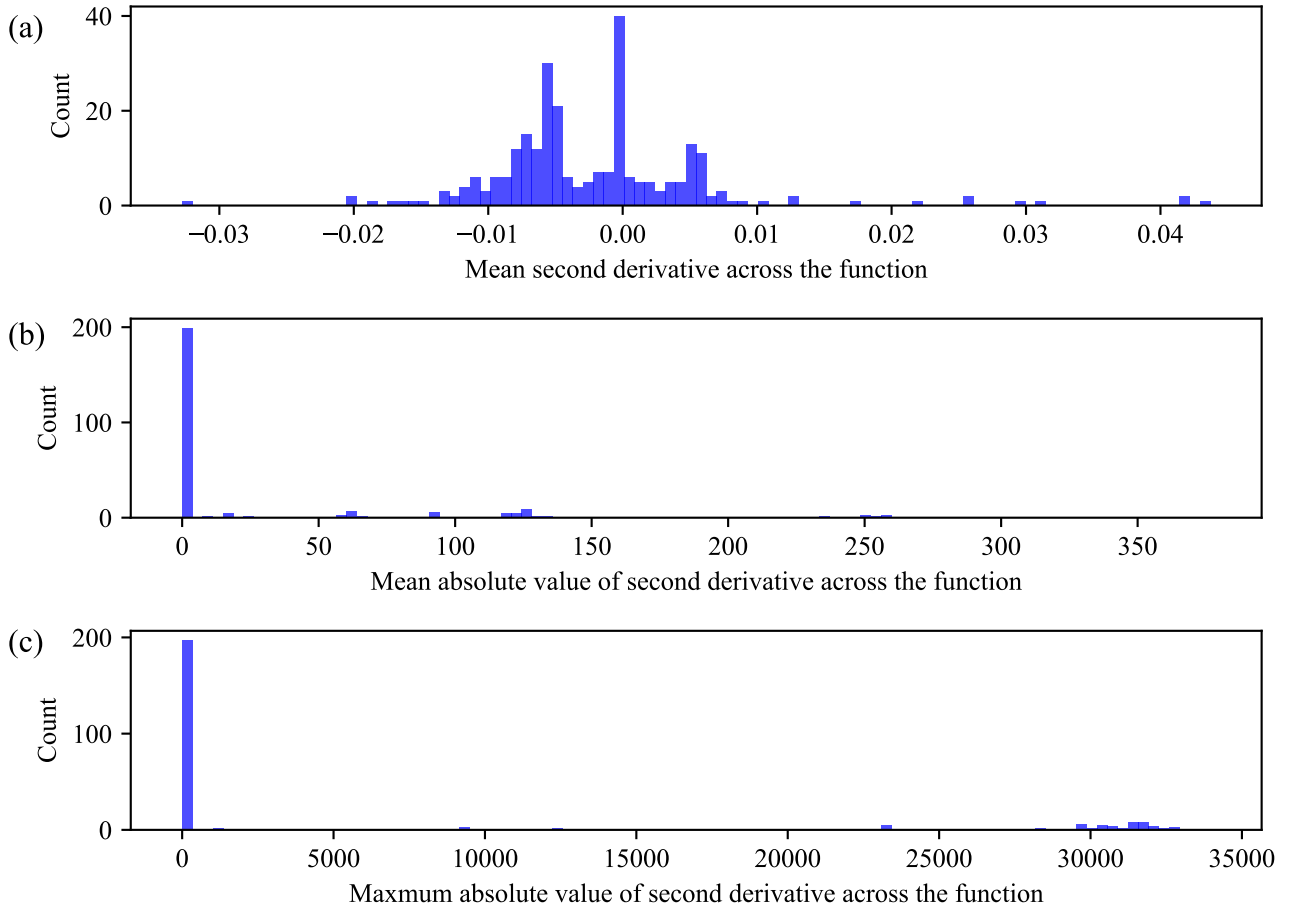


Figure 13. Distribution of second-order derivatives of functions $f_{s,(i,j)}|_{s_x}$. Unlike Figure 12, this figure only includes the subset of the functions that are neither linear nor JumpReLU-like. (a) The mean of the second-order derivative over the region of the input space. (b) The mean of the absolute value of the second-order derivative over the region of the input space. (c) The maximum value the second-order derivative takes in the region of the input space. Note that we are approximating the second derivative by looking at changes over a very small region (specifically 0.005), i.e. we do not take the limit as the size of this small region goes to zero; this is important because derivatives which would otherwise be undefined or infinite become finite with this approximation and therefore can be shown on the histograms. Also, we note that the means and maxima are taken over the region of the input space in which SAE features exist; see the footnote on page 15.

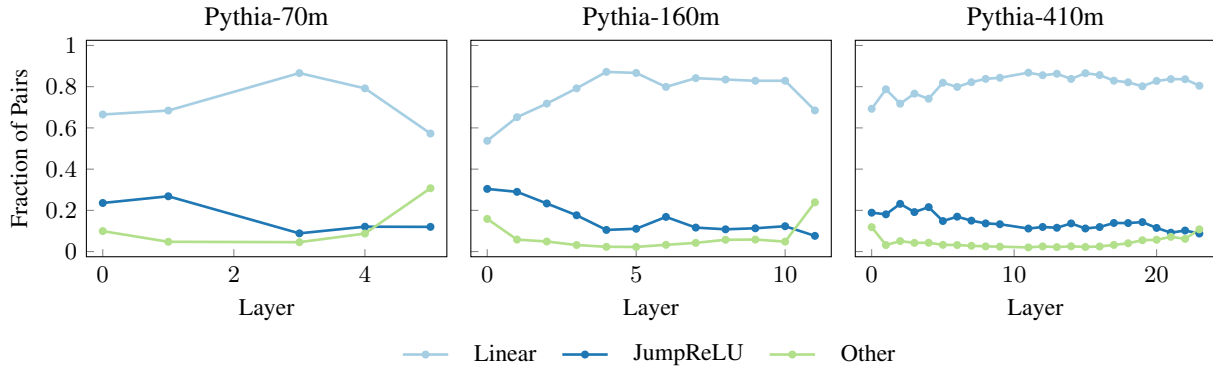


Figure 14. The fractions of Jacobian elements that exhibit a linear relationship between the input and output SAE latent activations, a JumpReLU-like relationship, and an uncategorized relationship, as described in Section 5.3. Here, we consider Jacobian SAEs trained on the feed-forward network at different layers of Pythia-70m, 160m, and 410m with fixed expansion factors $R = 64$ and $k = 32$. We computed the fractions over 1 million samples.

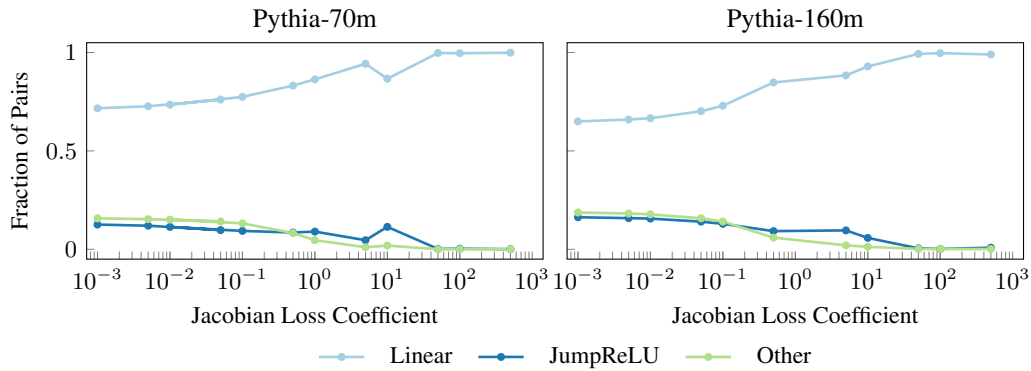


Figure 15. The fractions of Jacobian elements that exhibit a linear relationship between the input and output SAE latent activations, a JumpReLU-like relationship, and an uncategorized relationship, as described in Section 5.3. Here, we consider Jacobian SAEs trained on the feed-forward network at layer 3 of Pythia-70m (left) and layer 7 of Pythia-160m (right), with fixed expansion factors $R = 64$ and $k = 32$ and varying Jacobian loss coefficient (Section 4). We computed the fractions over 1 million samples.

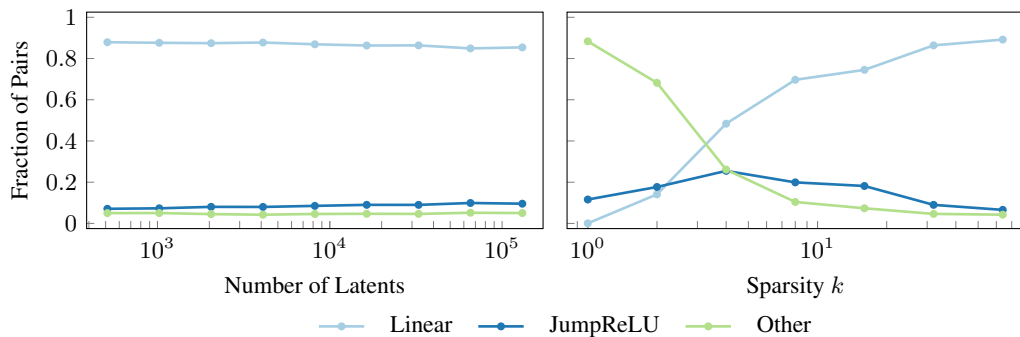


Figure 16. The fractions of Jacobian elements that exhibit a linear relationship between the input and output SAE latent activations, a JumpReLU-like relationship, and an uncategorized relationship, as described in Section 5.3. Here, we consider Jacobian SAEs trained on the feed-forward network at layer 3 of Pythia-70m with varying expansion factors (and hence numbers of latents; left) but fixed sparsities $k = 32$, and varying sparsities but fixed expansion factors $R = 64$ (Section 4). We computed the fractions over 1 million samples.

We can measure this more precisely by looking at the second-order derivative of $f_{s_{x,i,j}}|_{s_x}$. A zero second-order derivative across the whole domain would imply a linear function and, therefore, perfect predictive power of the Jacobian, while the larger the absolute value of the second-order derivative, the less predictive the Jacobian will be. This distribution is shown in Figure 12. The same distribution, which only includes the non-linear, non-JumpReLU functions, is shown in Figure 13. On average, the second derivative is extremely small for all features and effectively zero for the vast majority.

C. Training

Our training implementation is based on the open-source SAELens library (Bloom et al., 2024). We train each pair of SAEs on 300 million tokens from the Pile (Gao et al., 2020), excluding the copyrighted Books3 dataset, for a single epoch. Except where noted, we use a batch size of 4096 sequences, each with a context size of 2048. At a given time, we maintain 32 such batches of activation vectors in a buffer that is shuffled before training, which reduces variance in the training signal.

We use the Adam optimizer (Kingma & Ba, 2017) with the default beta parameters and a constant learning-rate schedule with 1% warm-up steps, 20% decay steps, and a maximum value of 5×10^{-4} . Additionally, we use 5% warm-up steps for the coefficient of the Jacobian term in the training loss. We initialize the decoder weight matrix to the transpose of the encoder, and we scale the decoder weight vectors to unit norm at initialization and after each training step (Gao et al., 2024).

Except where noted, we choose an expansion factor $R = 32$, keep the $k = 32$ largest latents in the TopK activation function of each of the input and output SAEs, and choose a coefficient of $\lambda = 1$ for the Jacobian term in the training loss.

C.1. Training signal stability

We initially considered the following setup:

$$s_x = e_x(\mathbf{x}), \quad \hat{\mathbf{x}} = d_x(s_x), \quad \mathbf{y} = f(\hat{\mathbf{x}}), \quad s_y = e_y(\mathbf{y}), \quad \hat{\mathbf{y}} = d_y(s_y) \quad (19)$$

The problem with this arrangement is that the second SAE depends on an output from the first SAE. Since both SAEs are trained simultaneously, we found that this compromised training signal stability – whenever the first SAE changed, the training distribution of the second SAE changed with it. Additionally, at the start of training, when the first SAE was not yet capable of outputting anything meaningful, the second SAE had no meaningful training data at all, which not only made it impossible for the second SAE to learn but also made the first SAE less stable via the Jacobian sparsity loss term.

To address this problem, we instead used this setup:

$$s_x = e_x(\mathbf{x}), \quad \hat{\mathbf{x}} = d_x(s_x), \quad \mathbf{y} = f(\mathbf{x}), \quad s_y = e_y(\mathbf{x}), \quad \hat{\mathbf{y}} = d_y(s_y) \quad (20)$$

Importantly, we pass the actual pre-MLP activations \mathbf{x} rather than the reconstructed activations $\hat{\mathbf{x}}$ into the MLP f . In addition to improving training stability, we believe this setup to be more faithful to the underlying model because both SAEs are trained on the unmodified activations that pass through the MLP.

D. Evaluation

We evaluated each of the input and output SAEs during training on ten batches of eight sequences, where each sequence has a context size of 2048, i.e., approximately 160K tokens. We computed the sparsity of the Jacobian, measured by the mean number of absolute values above 0.01 for a single token, separately after training. In this case, we collected statistics over 10 million tokens from the validation subset of the C4 text dataset.

For reconstruction quality, we report the mean cosine similarity between input activation vectors and their autoencoder reconstructions, the explained variance (MSE reconstruction error divided by the variance of the input activation vectors), and the MSE reconstruction error.

For model performance preservation, we report the cross-entropy loss score, which is the increase in the cross-entropy loss when the input activations are replaced by their autoencoder reconstruction divided by the increase in the loss when the input activations are ablated (set to zero).

³Note that we are testing whether functions are linear or JumpReLUs only in the region of input space within which SAE activations exist. In particular, this means that we are excluding negative numbers. More specifically, the domain within which we test the function’s structure is $[0, \max(5, s_{x,i}^{(l)} + 1)]$. In 92% of cases, $s_{x,i}^{(l)} + 1 < 5$; the median $s_{x,i}^{(l)}$ is 2.5.

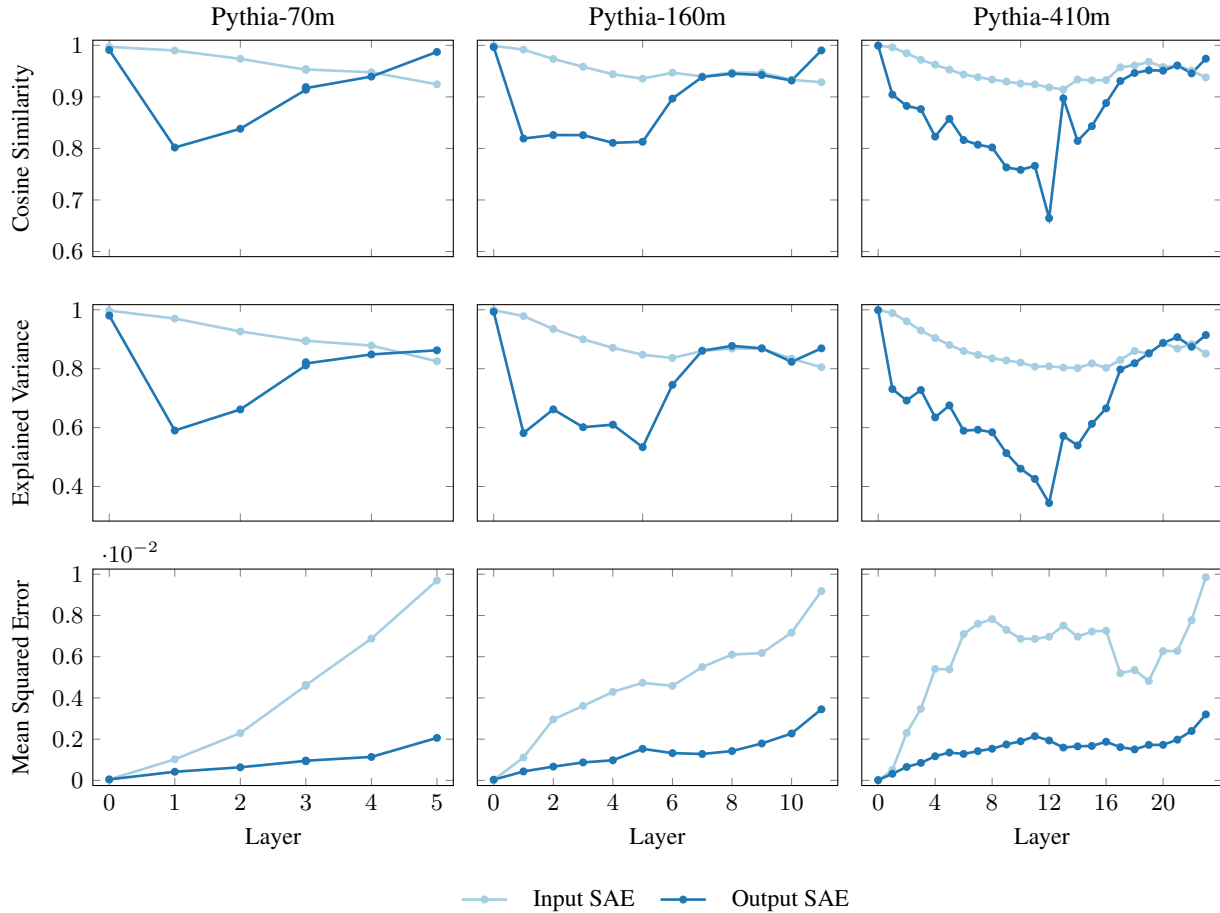


Figure 17. Reconstruction quality metrics for Jacobian SAEs trained on the feed-forward networks at every layer (residual block) of Pythia transformers. The cosine similarity is taken between the input and reconstructed activation vectors, and the explained variance is the MSE reconstruction error divided by the variance of the input activations. For each SAE, the expansion factor is $R = 64$ and $k = 32$; the Jacobian loss coefficient is 1.

For sparsity, we report the number of ‘dead’ latents that have not been activated (i.e., appeared in the k largest latents of the TopK activation function) within the preceding 10 million tokens during training and the number of latents that have activated fewer than once per 1 million tokens during training on average.

Given an expansion factor of 64, $k = 32$, and a Jacobian loss coefficient of 1, i.e., fixed hyperparameters, we find that the reconstruction error and cross-entropy loss score are consistently better for the input SAE than the output SAE. Additionally, we find that the performance is generally poorer for the intermediate layers than early and later layers.

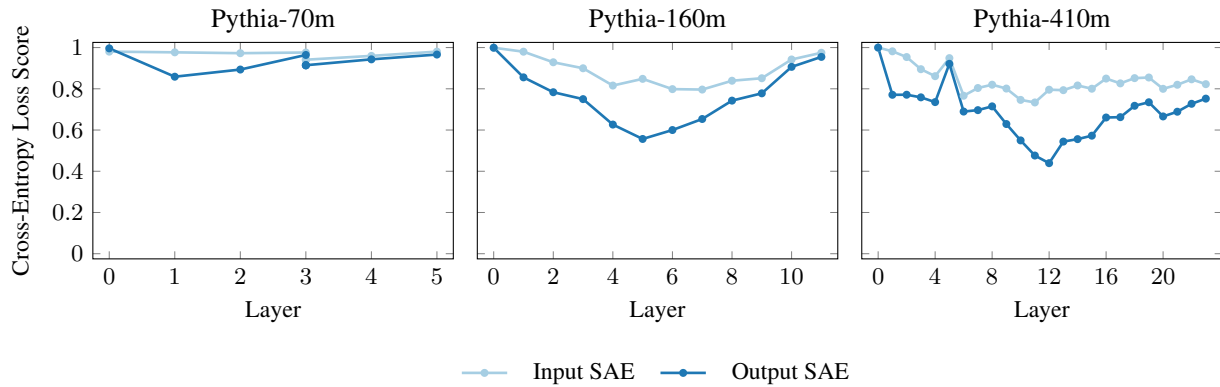


Figure 18. Model performance preservation metrics for Jacobian SAEs trained on the feed-forward networks at every layer (residual block) of Pythia transformers. The cross-entropy loss score is the increase in the cross-entropy loss when the input activations are replaced by their autoencoder reconstruction divided by the increase when the input activations are ablated (set to zero). For each SAE, the expansion factor is $R = 64$ and $k = 32$; the Jacobian loss coefficient is 1.

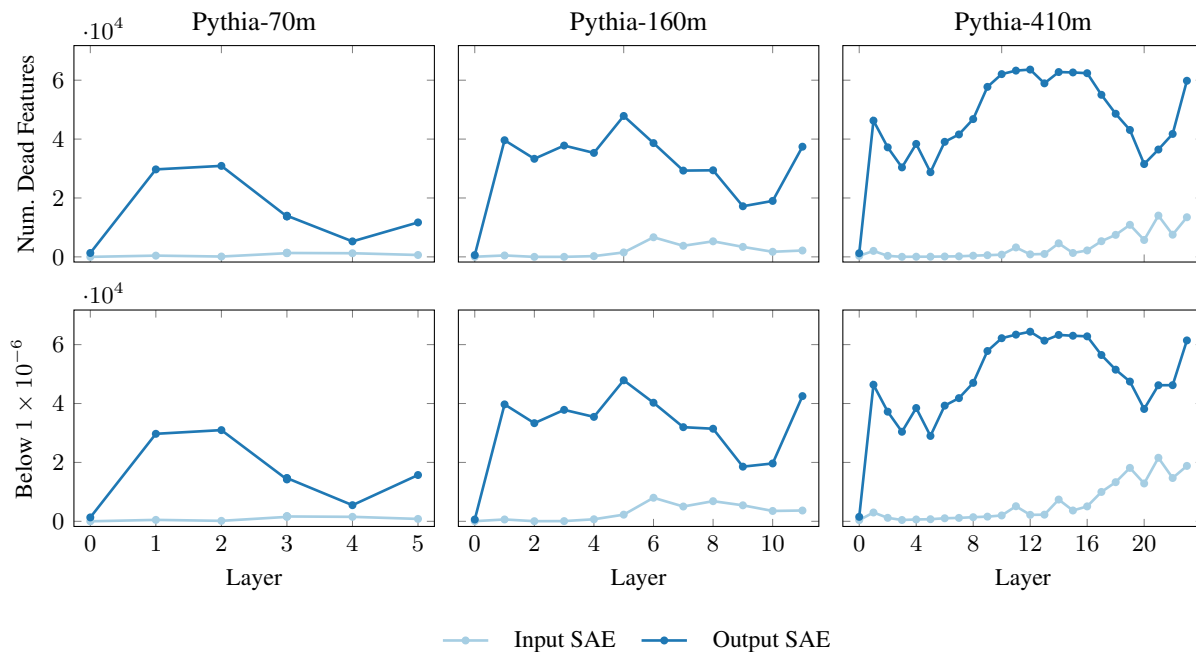


Figure 19. Sparsity metrics per layer for Jacobian SAEs trained on the feed-forward networks at every layer (residual block) of Pythia transformers. Recall that the L^0 norm per token for each of the input and output SAEs is fixed at k by the TopK activation function. For each SAE, the expansion factor is $R = 64$ and $k = 32$; the Jacobian loss coefficient is 1.

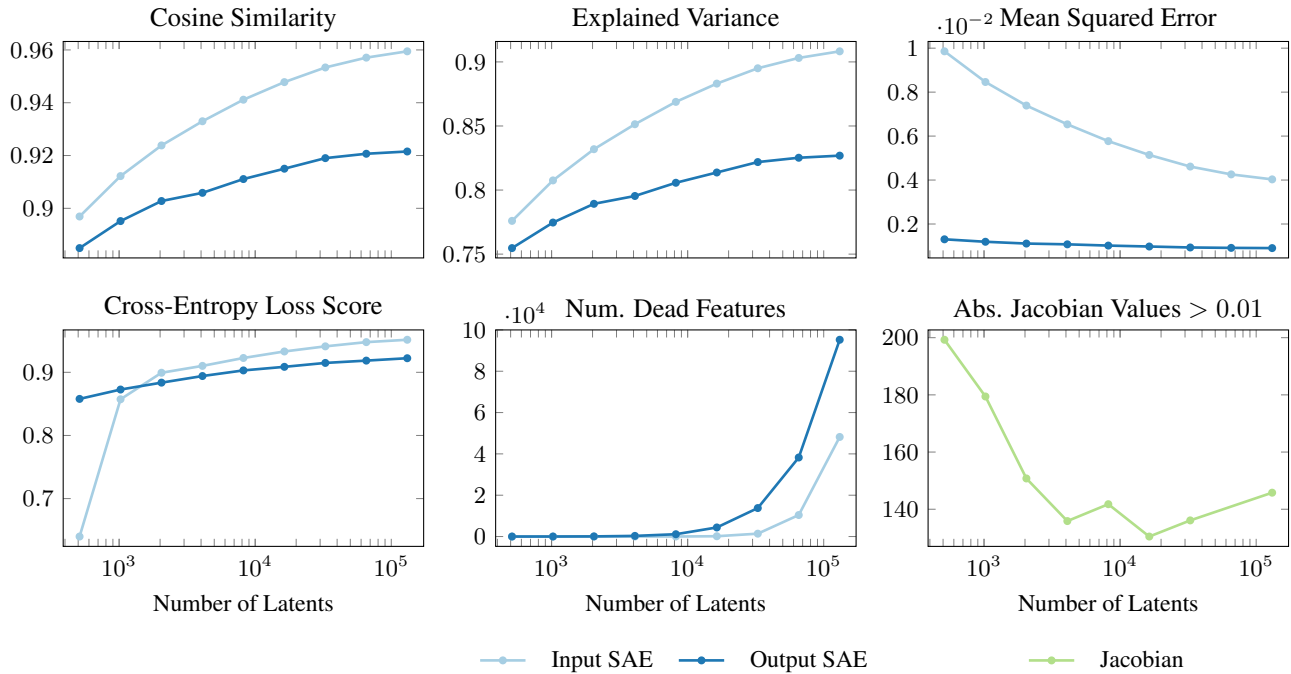


Figure 20. Reconstruction quality, model performance preservation, and sparsity metrics against the number of latents. Here, we consider Jacobian SAEs trained on the feed-forward network at layer 3 of Pythia-70m (model dimension 512) with $k = 32$. Recall that the maximum number of non-zero Jacobian values is $k^2 = 1024$. The reconstruction quality and cross-entropy loss score improve as the number of latents increases, and the number of dead features grows more quickly for the output SAE than the input SAE. See Appendix D for details of the evaluation metrics.

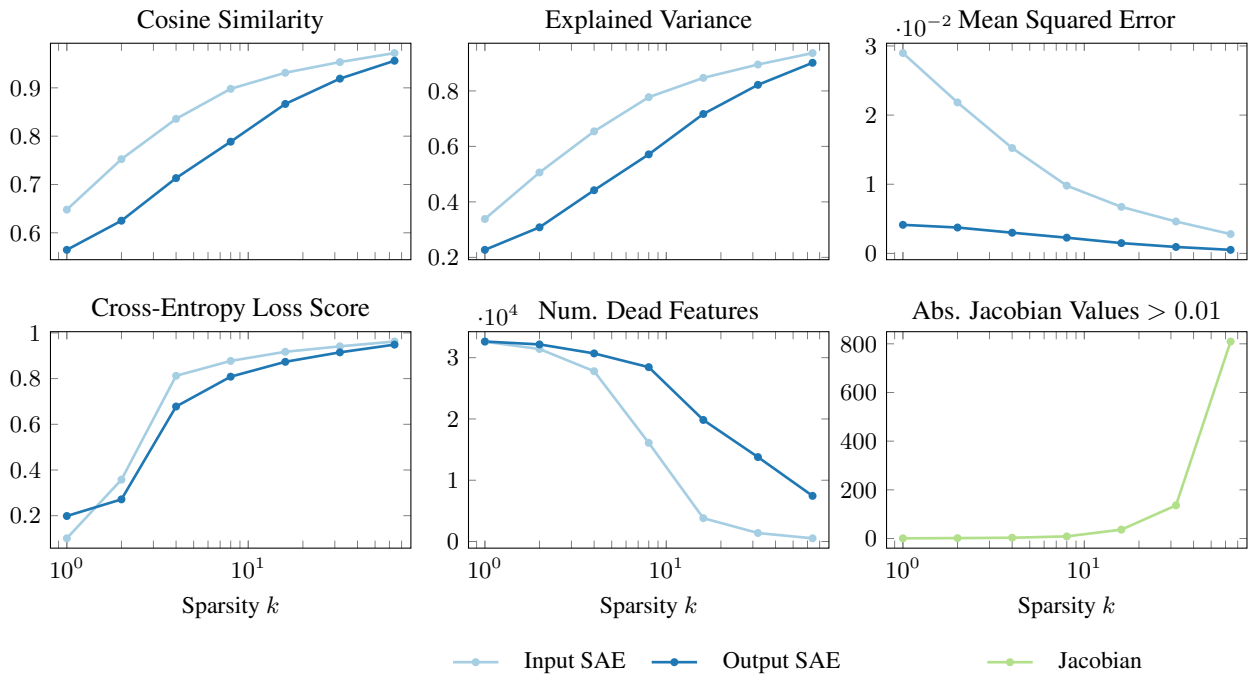


Figure 21. Reconstruction quality, model performance preservation, and sparsity metrics against the k largest latents to keep in the TopK activation function. Here, we consider Jacobian SAEs trained on the feed-forward network at layer 3 of Pythia-70m with expansion factor $R = 64$. Recall that the maximum number of non-zero Jacobian values is k^2 . The reconstruction quality and cross-entropy loss score improve as k increases, and the number of dead features decreases. See Appendix D for details of the evaluation metrics.

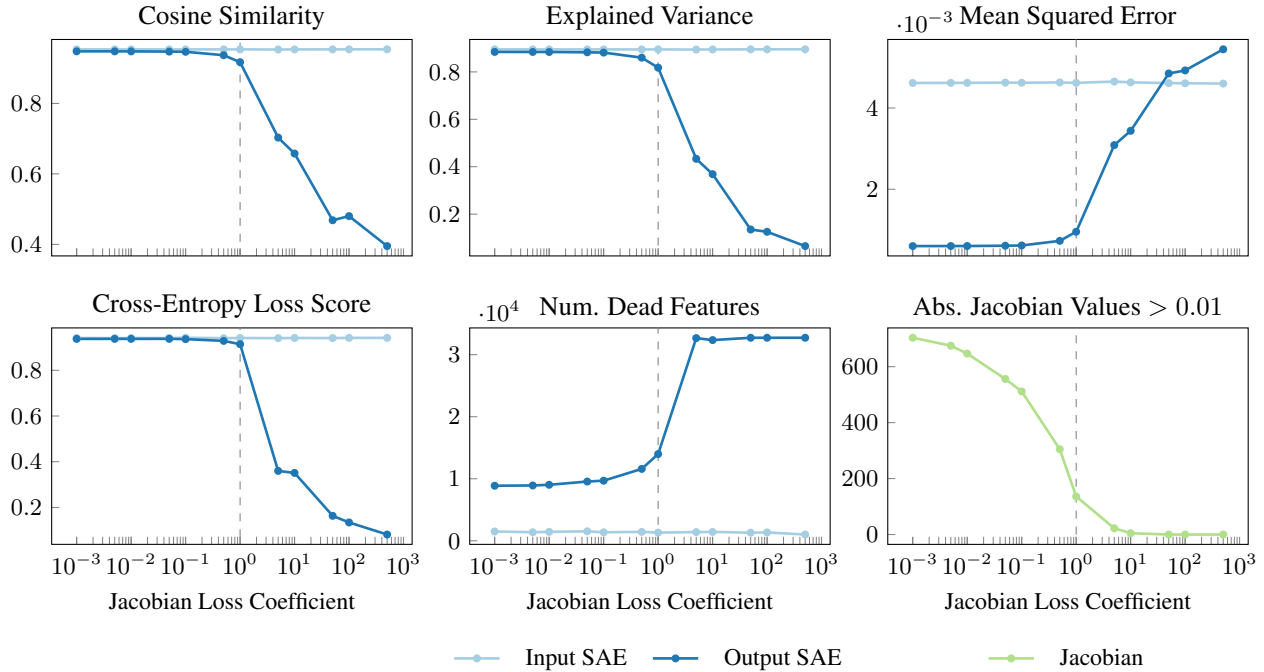


Figure 22. Reconstruction quality, model performance preservation, and sparsity metrics against the Jacobian loss coefficient. Here, we consider Jacobian SAEs trained on the feed-forward network at layer 3 of Pythia-70m with expansion factor $R = 64$ and $k = 32$. Recall that the maximum number of non-zero Jacobian values is $k^2 = 1024$. In accordance with Figure 4, all evaluation metrics degrade for values of the coefficient above 1. See Appendix D for details of the evaluation metrics.

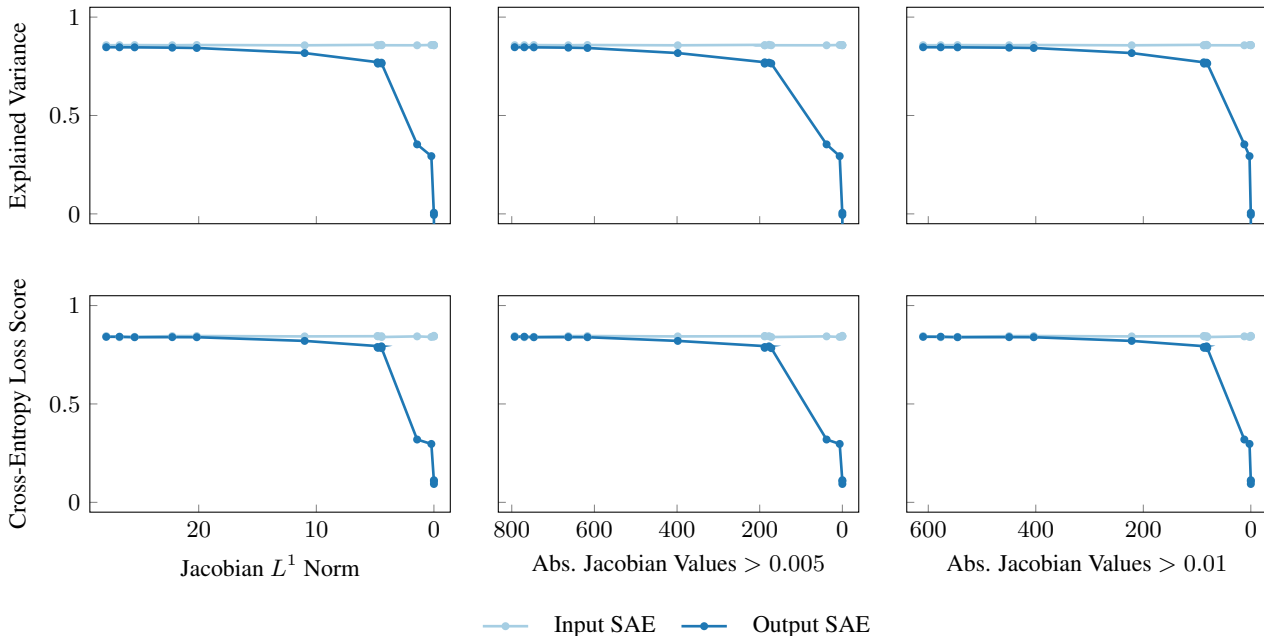


Figure 23. Pareto frontiers of the explained variance and cross-entropy loss score against different sparsity measures when varying the Jacobian loss coefficient. Here, we consider Jacobian SAEs trained on the feed-forward network at layer 3 of Pythia-70m with expansion factor $R = 64$ and $k = 32$. Recall that the maximum number of (dead) latents is 32768 (64 times the model dimension 512), and the maximum number of non-zero Jacobian values is $k^2 = 1024$. See Appendix D for details of the evaluation metrics.

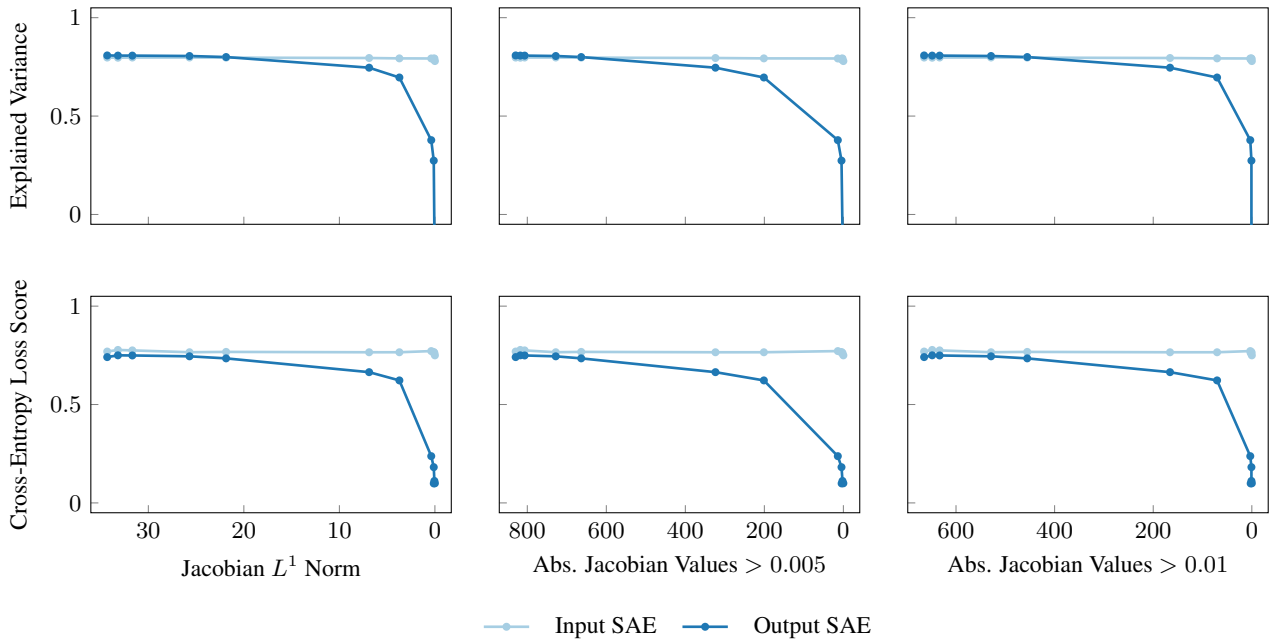


Figure 24. Pareto frontiers of the explained variance and cross-entropy loss score against different sparsity measures when varying the Jacobian loss coefficient. The coefficient has a relatively small impact on the reconstruction quality and sparsity of the input SAE, whereas it has a large effect on the sparsity of the output SAE and elements of the Jacobian matrix. Here, we consider Jacobian SAEs trained on the feed-forward network at layer 7 of Pythia-160m with expansion factor $R = 64$ and $k = 32$. Recall that the maximum number of (dead) latents is 49152 (64 times the model dimension 768), and the maximum number of non-zero Jacobian values is $k^2 = 1024$. See Appendix D for details of the evaluation metrics.

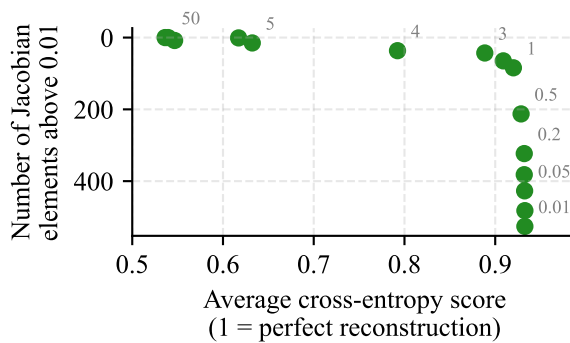


Figure 25. The trade-off between reconstruction quality and Jacobian sparsity as we vary the Jacobian loss coefficient. Each dot represents a pair of JSAEs trained with a specific Jacobian coefficient. Measured on layer 3 of Pythia-70m with $k = 32$.

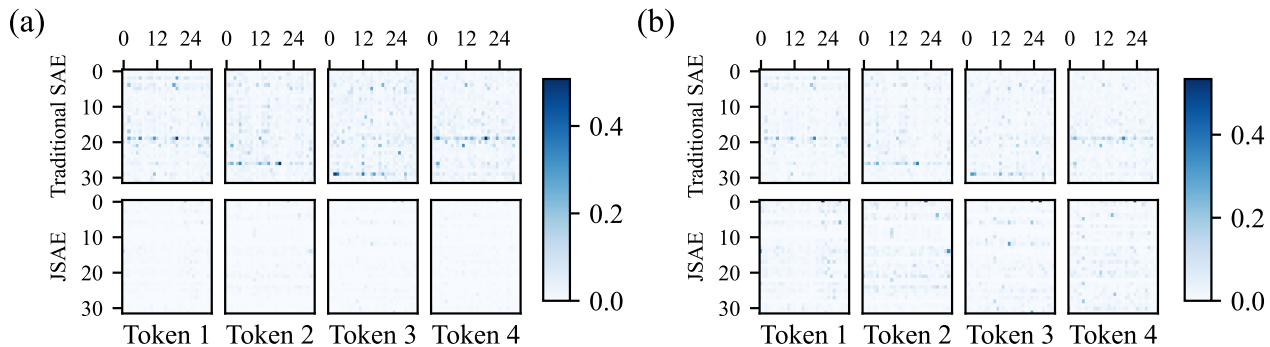


Figure 26. Comparison of Jacobians from traditional SAEs vs JSAEs, same as Figure 2 but with different normalization. (a) Not normalized. (b) L2 normalized. Measured on layer 15 of Pythia-410m.

We speculate that it is necessary to tune our hyperparameters for each layer individually to achieve improved performance; see, for example, Figures 22 and 3 for the variation of our evaluation metrics against the coefficient of the Jacobian loss term for individual layers of Pythia-70m and 160m.

E. More data on Jacobian sparsity

In Figure 19 we showed that Jacobians are much more sparse with JSAEs than traditional SAEs. To this end, we provided a representative example of what the Jacobians look like with JSAEs vs traditional SAEs. Some readers may object that this is not an apples-to-apples comparison since JSAEs are optimizing for lower L1 on the Jacobian, so it may be the case that JSAEs merely induce Jacobians with smaller elements, but their distribution may still be the same. To address this criticism, the examples are L2 normalized; we provide un-normalized versions as well as L1 normalized versions of the example Jacobians in Figure 26. We also provide a histogram and a CDF of the distribution of absolute values of Jacobian elements in Figure 28, which is taken across 10 million tokens.

E.1. Jacobian norms

In this section, we address an objection we expect some readers will have to our measures of sparsity. Our main metric for sparsity is the percentage of elements with absolute values above certain small thresholds (e.g. Figure 2). However, one can imagine two distributions with the same degree of sparsity, but vastly different results on this metric due to a different standard deviation. For instance, imagine two Gaussian distributions, both with $\mu = 0$ but with significantly different standard deviations, $\sigma_1 \gg \sigma_2$. They would score very differently on our metric, but their degrees of sparsity would not be meaningfully different (since sparsity requires there to be a small handful of relatively large elements). Since our L_1 penalty encourages the Jacobians to be smaller, it could be that they simply become more tightly clustered around 0. However, this is not the case. We can measure this by looking at the "norms" of the Jacobian, i.e. we flatten the Jacobian, treat it as a vector, and compute its L_p norms. If the Jacobian is merely becoming smaller, we would expect all of its L_p norms to decrease at roughly the same rate. On the other hand, if the Jacobian is becoming sparser, we would expect its L_1, L_2 norms to decrease while its L_4, \dots, L_∞ norms, which depend more strongly on the presence or absence of a few large elements, should stay roughly the same. We present these results in Figure 31, as we can see, the Jacobian does become slightly smaller, but most of the effect we see is indeed the Jacobian becoming significantly more sparse.

F. Interpreting Jacobian elements by examples

A common approach to interpreting language-model components such as neurons is to collect token sequences and the corresponding activations over a text dataset (e.g., Yun et al., 2021; Bills et al., 2023). The maximal latent activations may be retained, or activations from different quantiles of the distribution over the dataset (Bricken et al., 2023; Choi et al., 2024; Paulo et al., 2024). With Jacobian SAEs, there are several types of activations that we could collect and from which we could retain (e.g.) the maximum positive values to interpret SAE latents: the latent activations of the input SAE, the latent activations of the output SAE, and the elements of the Jacobian matrix between the input and output SAE latents.

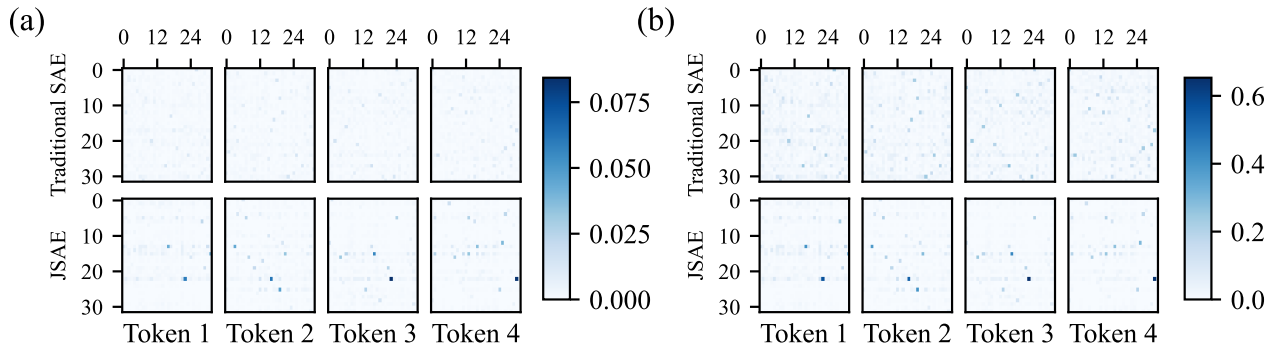


Figure 27. Comparison of Jacobians from traditional SAEs vs JSAEs, same as Figure 2 but with different normalization. (a) L1 normalized. (b) L2 normalized. Measured on layer 3 of Pythia-70m.

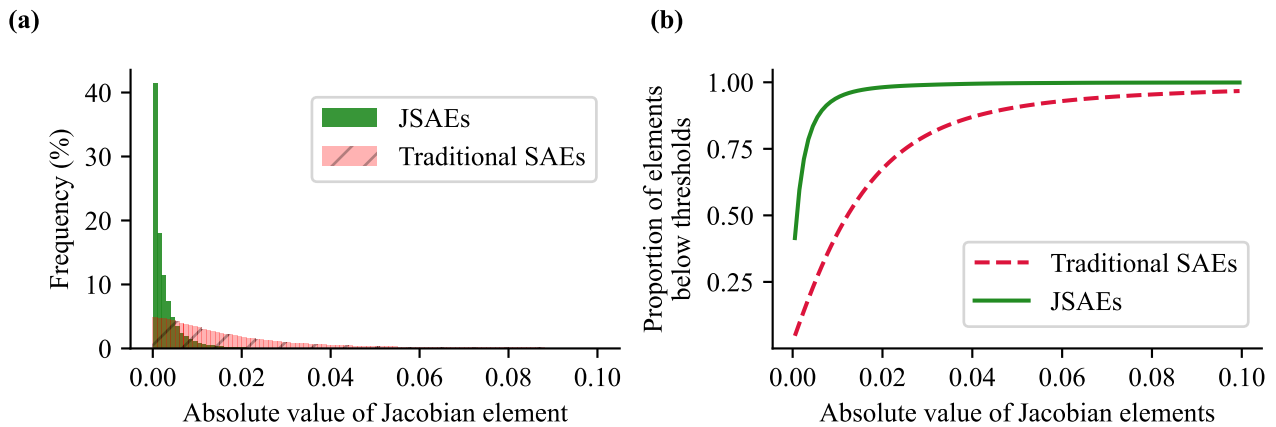


Figure 28. Further data showing that JSAEs induce much greater Jacobian sparsity than traditional SAEs. (a) A histogram of the absolute values of Jacobian elements in JSAEs versus traditional SAEs. JSAEs induce significantly more sparse Jacobians than standard SAEs. This means that there is a relatively small number of input-output feature pairs which explain a very large fraction of the computation being performed. Note that only the $k \times k$ elements corresponding to active latents are included in the histogram – the remaining $(n_y - k) \times (n_x - k)$ elements are zero by definition both for JSAEs and standard TopK SAEs. The histogram was collected over 10 million tokens from the validation subset of the C4 text dataset, which produced 10.24 billion feature pairs. (b) The cumulative distribution function of the absolute values of Jacobian elements, again demonstrating that JSAEs induce significantly more computational sparsity than traditional SAEs. Measured on layer 15 of Pythia-410m.

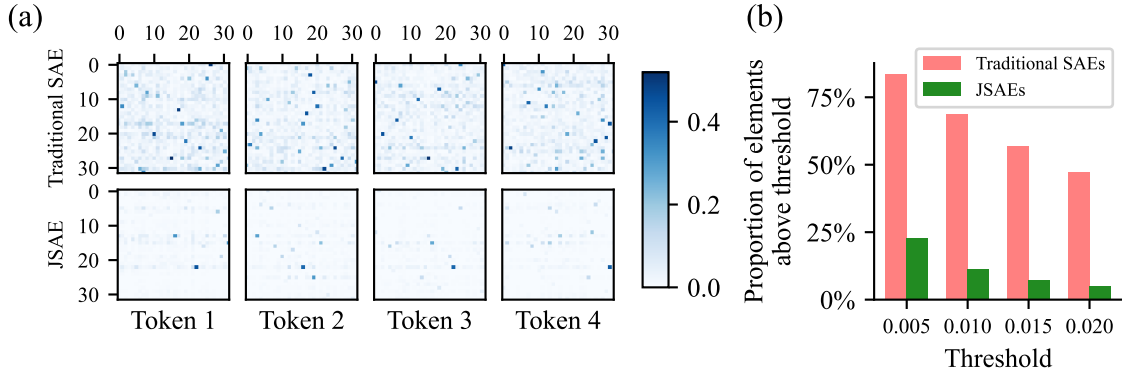


Figure 29. JSAs induce a much greater degree of sparsity in the elements of the Jacobian than traditional SAEs. Identical to Figure 2 but measured on layer 3 of Pythia-70m.

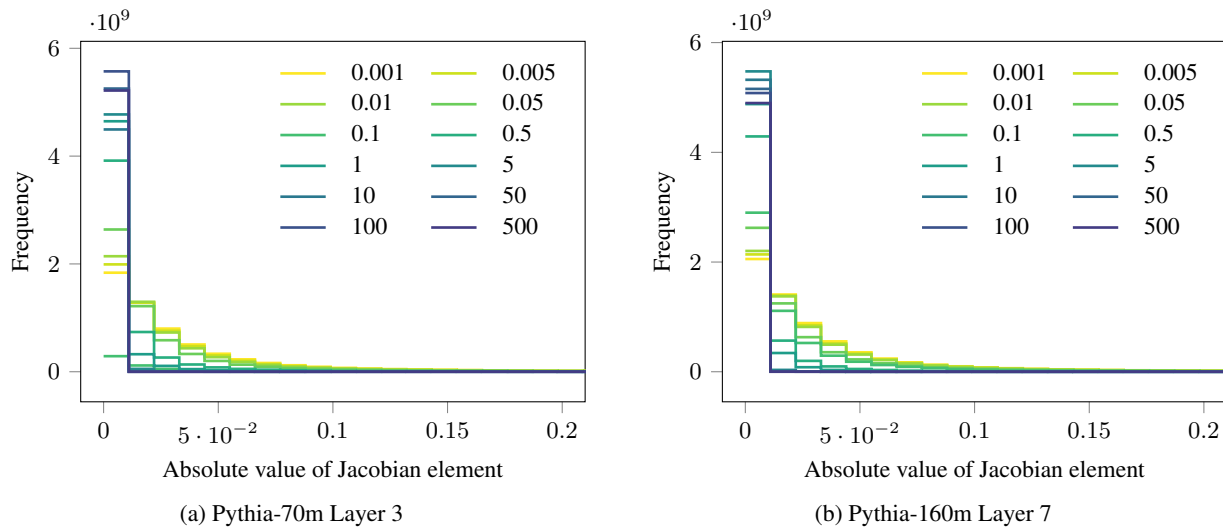


Figure 30. Histograms that show the frequency of absolute values of non-zero Jacobian elements for different values of the coefficient of the Jacobian loss term. As the coefficient increases, the frequency of larger values decreases, i.e., the Jacobian becomes sparser. We provide further details in Figure 28.

Intuitively, we expected to find correlations between the j -th input SAE latent activation, the i -th output SAE latent activation, and the (i, j) -th element of the Jacobian matrix. However, for Pythia-70m and a small sample of 10K tokens, the Pearson correlation coefficients between these pairs of values were mostly small, on the order of 0.1. Hence, we chose to collect the input and output SAE latent activations alongside the elements of the Jacobian. Specifically, for each model, we began by collecting summary statistics for each non-zero element of the Jacobian matrix and the corresponding input and output SAE latent activations (Table 1), over the first 10K records of the English subset of the C4 text dataset (Raffel et al., 2020). Given these summary statistics, we found the top 32 pairs of input and output SAE latent indices when the statistics for each pair were sorted in descending order of the mean absolute value of non-zero Jacobian elements.

For each of these pairs, we collected the input and output SAE latent activations and Jacobian elements over examples of context length 16 from the same text dataset, retaining examples where at least one token produced a non-zero Jacobian element. We chose a context length of 16 to conveniently display examples and retained the top eight examples when sorted in descending order of the maximum Jacobian element over the example. Each table of examples displays a list of at most 12 examples, each comprising 16 tokens; we exclude the end-of-sentence token for brevity. The values of non-zero Jacobian elements and the activations of the corresponding input and output SAE latent indices are indicated by the opacity of the background color for each token. We take the opacity to be the element or activation divided by the maximum value over the dataset, i.e., all the examples with a non-zero Jacobian element for a given pair of input and output SAE latent indices. For clarity, we report the maximum element or activation alongside the colored tokens. Tables 2, 3, 4, 5, and 6 were chosen from among the pairs of latent indices with the top 32 maximum mean absolute values of Jacobian elements over the dataset to broadly demonstrate the patterns we observed within latent activations and Jacobian elements.

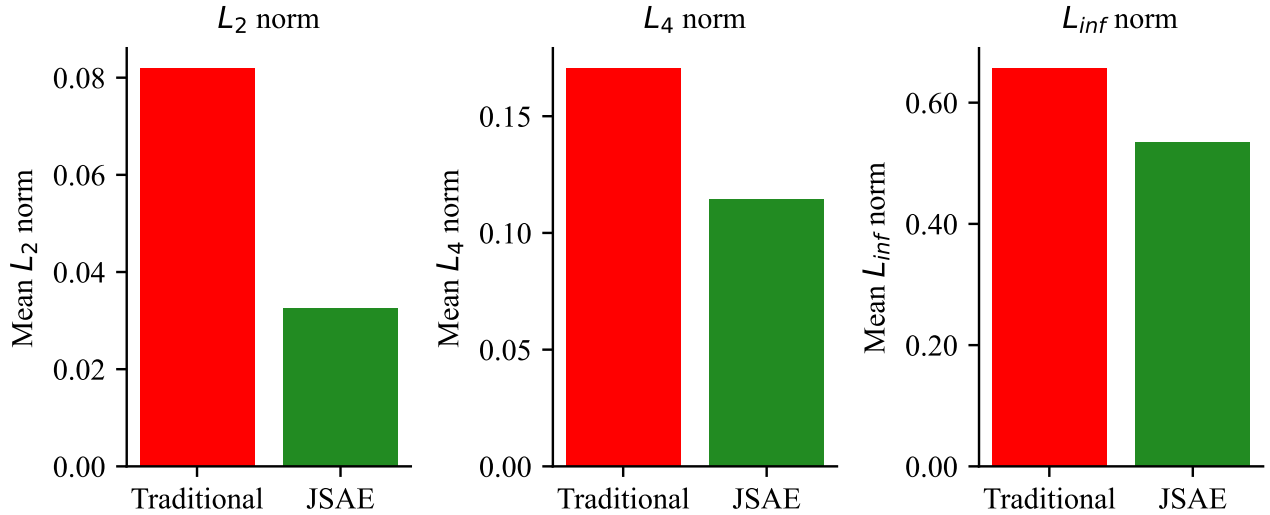


Figure 31. L_p norms of the Jacobians. We measure these by flattening the Jacobians and treating them as a vector. These results imply that the Jacobians are in fact becoming much more sparse, as opposed to merely becoming smaller (see Section E.1). Averaged across 1 million tokens, measured on layer 4 of Pythia-70m.

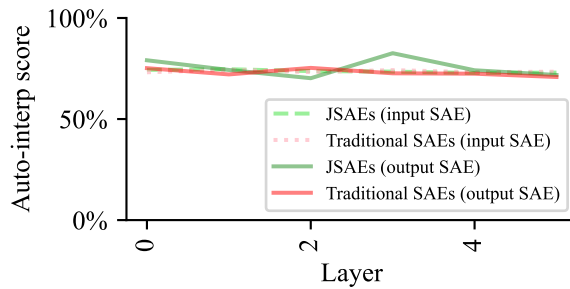


Figure 32. Automatic interpretability scores of JSAs are very similar to traditional SAs. Measured on all layers of Pythia-70m using the “fuzzing” scorer from Paulo et al. (2024).

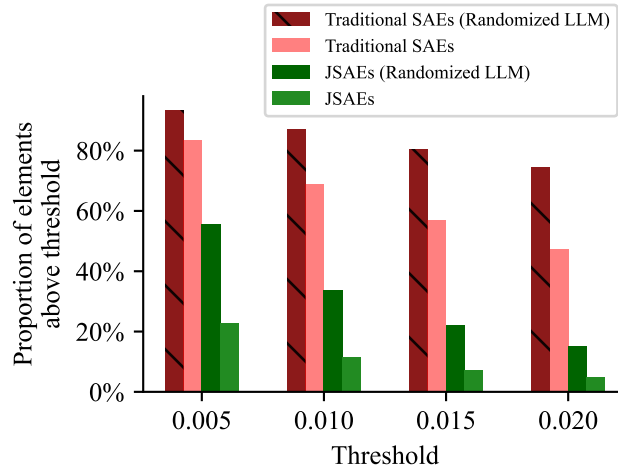


Figure 33. Jacobians are substantially more sparse in pre-trained LLMs than in randomly initialized transformers. This holds both when you actively optimize for Jacobian sparsity with JSAEs, and when you don’t optimize for it and use traditional SAEs. The proportion of Jacobian elements with absolute values above certain thresholds. The figure shows the proportion of Jacobian elements with absolute values above certain thresholds. Identical to Figure 6 but measured on layer 3 of Pythia-70m.

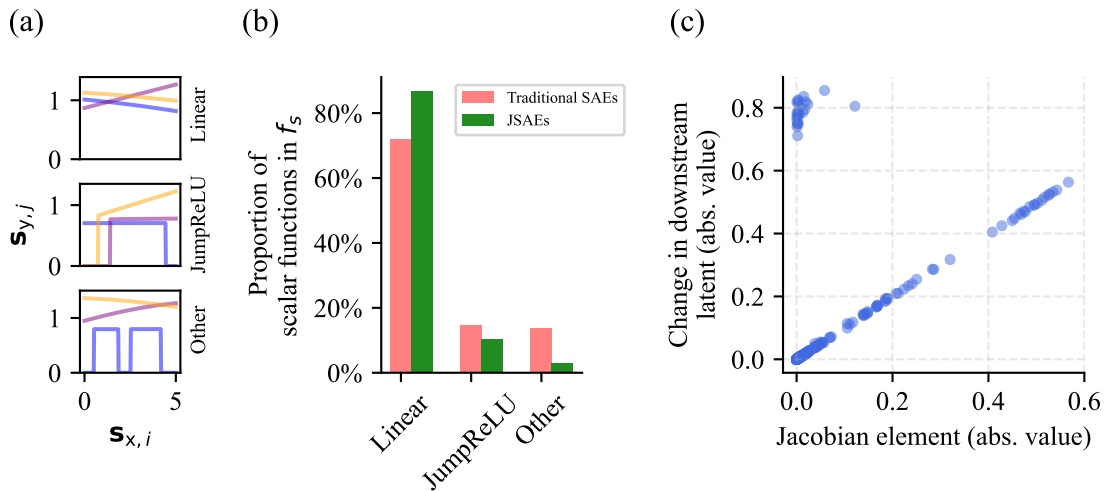


Figure 34. The function f_s , which combines the decoder of the first SAE, the MLP, and the encoder of the second SAE, is mostly linear. Identical to Figure 7 but measured on layer 3 of Pythia-70m.

Statistic for Latent Index Pairs	Median	Mean	Standard Deviation
Count	$3.00 \cdot 10^0$	$1.79 \cdot 10^2$	$5.85 \cdot 10^3$
Mean	$-1.40 \cdot 10^{-3}$	$-2.20 \cdot 10^{-3}$	$1.93 \cdot 10^{-2}$
Standard Deviation	$2.20 \cdot 10^{-3}$	$4.05 \cdot 10^{-3}$	$5.32 \cdot 10^{-3}$
Mean Absolute Value	$8.67 \cdot 10^{-3}$	$1.33 \cdot 10^{-2}$	$1.47 \cdot 10^{-2}$
Standard Deviation of Absolute Values	$1.77 \cdot 10^{-3}$	$3.26 \cdot 10^{-3}$	$4.31 \cdot 10^{-3}$

(a) Pythia-70m, Layer 3

Statistic for Latent Index Pairs	Median	Mean	Standard Deviation
Count	$2.00 \cdot 10^0$	$6.34 \cdot 10^1$	$2.29 \cdot 10^3$
Mean	$-7.90 \cdot 10^{-4}$	$-3.81 \cdot 10^{-4}$	$1.05 \cdot 10^{-2}$
Standard Deviation	$1.12 \cdot 10^{-3}$	$2.10 \cdot 10^{-3}$	$3.00 \cdot 10^{-3}$
Mean Absolute Value	$4.46 \cdot 10^{-3}$	$7.16 \cdot 10^{-3}$	$8.04 \cdot 10^{-3}$
Standard Deviation of Absolute Values	$8.69 \cdot 10^{-4}$	$1.66 \cdot 10^{-3}$	$2.39 \cdot 10^{-3}$

(b) Pythia-160m, Layer 7

Statistic for Latent Index Pairs	Median	Mean	Standard Deviation
Count	$6.00 \cdot 10^0$	$1.19 \cdot 10^2$	$2.15 \cdot 10^3$
Mean	$-2.34 \cdot 10^{-4}$	$-5.51 \cdot 10^{-4}$	$3.78 \cdot 10^{-3}$
Standard Deviation	$2.58 \cdot 10^{-4}$	$8.65 \cdot 10^{-4}$	$1.60 \cdot 10^{-3}$
Mean Absolute Value	$6.76 \cdot 10^{-4}$	$1.90 \cdot 10^{-3}$	$3.52 \cdot 10^{-3}$
Standard Deviation of Absolute Values	$1.98 \cdot 10^{-4}$	$6.54 \cdot 10^{-4}$	$1.22 \cdot 10^{-3}$

(c) Pythia-410m, Layer 15

Table 1. The mean and standard deviation over pairs of input and output SAE latent indices, i.e., non-zero elements of the Jacobian matrix, for different summary statistics of each pair. The statistics were collected over the first 10K records of the English subset of the C4 text dataset (Raffel et al., 2020). The standard deviation in the count of non-zero Jacobian elements is very large, i.e., the frequency with which pairs of latent indices are non-zero varies widely. For each underlying transformer and MLP layer, the Jacobian SAE pair was trained with an expansion factor of $R = 64$ and sparsity $k = 32$.

Category	Max. abs. value	Example tokens
Jacobian	3.993×10^{-1}	. I didn ' t ask for them . I didn ' t see them
Input SAE	1.937×10^1	. I didn ' t ask for them . I didn ' t see them
Output SAE	6.176	. I didn ' t ask for them . I didn ' t see them
Jacobian	3.947×10^{-1}	by minute basis . It ' s easy for someone to come along who isn
Input SAE	1.677×10^1	by minute basis . It ' s easy for someone to come along who isn
Output SAE	5.698	by minute basis . It ' s easy for someone to come along who isn
Jacobian	3.937×10^{-1}	! I ' m glad it worked partially for you although it didn
Input SAE	1.806×10^1	! I ' m glad it worked partially for you although it didn
Output SAE	6.157	! I ' m glad it worked partially for you although it didn
Jacobian	3.931×10^{-1}	read other books then the Bible , but if the Bible isn ' t being
Input SAE	2.153×10^1	read other books then the Bible , but if the Bible isn ' t being
Output SAE	7.214	read other books then the Bible , but if the Bible isn ' t being
Jacobian	3.930×10^{-1}	hide her pills in) . She didn ' t like it . She also didn
Input SAE	1.971×10^1	hide her pills in) . She didn ' t like it . She also didn
Output SAE	6.299	hide her pills in) . She didn ' t like it . She also didn
Jacobian	3.925×10^{-1}	breakdown s that day because I couldn ' t connect with him . I couldn
Input SAE	1.977×10^1	breakdown s that day because I couldn ' t connect with him . I couldn
Output SAE	6.820	breakdown s that day because I couldn ' t connect with him . I couldn
Jacobian	3.907×10^{-1}	you . Kot lin is like a Java cousin with better looks and who doesn
Input SAE	2.208×10^1	you . Kot lin is like a Java cousin with better looks and who doesn
Output SAE	7.360	you . Kot lin is like a Java cousin with better looks and who doesn
Jacobian	3.906×10^{-1}	found a nice copy used . Unfortunately , I didn ' t like it very
Input SAE	2.139×10^1	found a nice copy used . Unfortunately , I didn ' t like it very
Output SAE	7.267	found a nice copy used . Unfortunately , I didn ' t like it very
Jacobian	3.902×10^{-1}	the story they told themselves about their failures was , " well aG I couldn
Input SAE	2.136×10^1	the story they told themselves about their failures was , " well aG I couldn
Output SAE	7.384	the story they told themselves about their failures was , " well aG I couldn
Jacobian	3.894×10^{-1}	. But the last 50 pages or so are brilliant . I couldn ' t
Input SAE	1.966×10^1	. But the last 50 pages or so are brilliant . I couldn ' t
Output SAE	6.700	. But the last 50 pages or so are brilliant . I couldn ' t
Jacobian	3.890×10^{-1}	reminding me that this is technical manual and that it didn ' t need to be
Input SAE	2.161×10^1	reminding me that this is technical manual and that it didn ' t need to be
Output SAE	7.011	reminding me that this is technical manual and that it didn ' t need to be
Jacobian	3.889×10^{-1}	and look forward to many more . Don ' t tell me that diversity doesn
Input SAE	1.910×10^1	and look forward to many more . Don ' t tell me that diversity doesn
Output SAE	6.600	and look forward to many more . Don ' t tell me that diversity doesn

Table 2. The top 12 examples that produce the maximum absolute values of the Jacobian element with input SAE latent index 24720 and output latent index 33709. The Jacobian SAE pair was trained on layer 15 of Pythia-410m with an expansion factor of $R = 64$ and sparsity $k = 32$. The examples were collected over the first 10K records of the English subset of the C4 text dataset (Raffel et al., 2020), with a context length of 16 tokens. For each example, the first row shows the values of the Jacobian element, and the second and third show the corresponding activations of the input and output SAE latents. In this case, both SAE latents appear to activate for tokens immediately preceding ' t that form negative contractions in English.

Jacobian Sparse Autoencoders: Sparsify Computations, Not Just Activations

Category	Max. abs. value	Example tokens
Jacobian	3.349×10^{-1}	confirm that there was nothing else it needed to disclose ." B LC Press Release
Input SAE	5.743×10^{-1}	confirm that there was nothing else it needed to disclose ." B LC Press Release
Output SAE	4.708	confirm that there was nothing else it needed to disclose ." B LC Press Release
Jacobian	3.348×10^{-1}	Example : The integral electronic control unit ver ifies whether there is indeed a sol
Input SAE	2.363	Example : The integral electronic control unit ver ifies whether there is indeed a sol
Output SAE	4.998	Example : The integral electronic control unit ver ifies whether there is indeed a sol
Jacobian	3.342×10^{-1}	see that there is a ton of old fishing line out there floating around .
Input SAE	5.289×10^{-1}	see that there is a ton of old fishing line out there floating around .
Output SAE	4.801	see that there is a ton of old fishing line out there floating around .
Jacobian	3.335×10^{-1}	. Maybe you won ' t believe it , but in present , there
Input SAE	8.741×10^{-1}	. Maybe you won ' t believe it , but in present , there
Output SAE	4.742	. Maybe you won ' t believe it , but in present , there
Jacobian	3.334×10^{-1}	virus indicates that there may be important amino acid co - sub stit utions in
Input SAE	7.625	virus indicates that there may be important amino acid co - sub stit utions in
Output SAE	4.617	virus indicates that there may be important amino acid co - sub stit utions in
Jacobian	3.333×10^{-1}	ensure that there would be a sufficient reserve to avoid un - staff ed routes
Input SAE	7.634	ensure that there would be a sufficient reserve to avoid un - staff ed routes
Output SAE	4.676	ensure that there would be a sufficient reserve to avoid un - staff ed routes
Jacobian	3.327×10^{-1}	wire cage , ensure that there are no bits of wire p oking out that
Input SAE	7.182×10^{-1}	wire cage , ensure that there are no bits of wire p oking out that
Output SAE	4.662	wire cage , ensure that there are no bits of wire p oking out that
Jacobian	3.326×10^{-1}	it is important to study if there is one approach that you use more often
Input SAE	6.788×10^{-1}	it is important to study if there is one approach that you use more often
Output SAE	4.480	it is important to study if there is one approach that you use more often
Jacobian	3.322×10^{-1}	, that there is no point in trying to understand any users at all .
Input SAE	4.728×10^{-1}	, that there is no point in trying to understand any users at all .
Output SAE	4.607	, that there is no point in trying to understand any users at all .
Jacobian	3.318×10^{-1}	Now that there is known information , everything feels like it is within reach .
Input SAE	9.027×10^{-1}	Now that there is known information , everything feels like it is within reach .
Output SAE	4.570	Now that there is known information , everything feels like it is within reach .
Jacobian	3.315×10^{-1}	seen that there is a wealth of un ta pped talent here . Some
Input SAE	6.374×10^{-1}	seen that there is a wealth of un ta pped talent here . Some
Output SAE	4.643	seen that there is a wealth of un ta pped talent here . Some
Jacobian	3.315×10^{-1}	If there ' s one that you like , you can stick your face through
Input SAE	5.826×10^{-1}	If there ' s one that you like , you can stick your face through
Output SAE	4.453	If there ' s one that you like , you can stick your face through

Table 3. The top 12 examples that produce the maximum absolute values of the Jacobian element with input SAE latent index 314 and output latent index 31729. The Jacobian SAE pair was trained on layer 15 of Pythia-410m with an expansion factor of $R = 64$ and sparsity $k = 32$. The examples were collected over the first 10K records of the English subset of the C4 text dataset (Raffel et al., 2020), with a context length of 16 tokens. For each example, the first row shows the values of the Jacobian element, and the second and third show the corresponding activations of the input and output SAE latents. In this case, the input SAE latent appears to weakly activate for the token ‘there’ and strongly activate for modal auxiliary verbs following ‘there’ (i.e., ‘may’ and ‘would’), whereas the output SAE latent appears to activate for both tokens.

Category	Max. abs. value	Example tokens
Jacobian	2.788×10^{-1}	flood barrier (Gre if sw ald , Germany). The b MC Team
Input SAE	1.121	flood barrier (Gre if sw ald , Germany). The b MC Team
Output SAE	5.615×10^{-1}	flood barrier (Gre if sw ald , Germany). The b MC Team
Jacobian	2.773×10^{-1}	Center . Her works have also been produced at Ste ppen wolf Theatre Company ,
Input SAE	2.075	Center . Her works have also been produced at Ste ppen wolf Theatre Company ,
Output SAE	9.516×10^{-1}	Center . Her works have also been produced at Ste ppen wolf Theatre Company ,
Jacobian	2.773×10^{-1}	102 S A nt is 250 3 m 2021 m 1 150 m Switzerland
Input SAE	1.529	102 S A nt is 250 3 m 2021 m 1 150 m Switzerland
Output SAE	1.039	102 S A nt is 250 3 m 2021 m 1 150 m Switzerland
Jacobian	2.772×10^{-1}	K ont ak B BM Mur ah Berg ar ans i How to communication
Input SAE	1.235	K ont ak B BM Mur ah Berg ar ans i How to communication
Output SAE	8.479×10^{-1}	K ont ak B BM Mur ah Berg ar ans i How to communication
Jacobian	2.767×10^{-1}	get quality care and all hospitals in Berg en County will see less traffic in
Input SAE	3.480	get quality care and all hospitals in Berg en County will see less traffic in
Output SAE	8.445×10^{-1}	get quality care and all hospitals in Berg en County will see less traffic in
Jacobian	2.753×10^{-1}	Pay . Car amel eggs by Cad bury UK , available at Eng en
Input SAE	1.189	Pay . Car amel eggs by Cad bury UK , available at Eng en
Output SAE	6.593×10^{-1}	Pay . Car amel eggs by Cad bury UK , available at Eng en
Jacobian	2.749×10^{-1}	of the ER by providing free , ongoing primary care to residents of Berg en
Input SAE	3.194	of the ER by providing free , ongoing primary care to residents of Berg en
Output SAE	1.024	of the ER by providing free , ongoing primary care to residents of Berg en
Jacobian	2.744×10^{-1}	. C reme egg by Cad bury UK , available at Eng en .
Input SAE	1.206	. C reme egg by Cad bury UK , available at Eng en .
Output SAE	6.785×10^{-1}	. C reme egg by Cad bury UK , available at Eng en .
Jacobian	2.736×10^{-1}	. O reo filled eggs by Cad bury UK , available at Eng en
Input SAE	1.260	. O reo filled eggs by Cad bury UK , available at Eng en
Output SAE	6.371×10^{-1}	. O reo filled eggs by Cad bury UK , available at Eng en
Jacobian	2.735×10^{-1}	Car ls bad horse owner and handic apper Jon Lind o reinforced Santa An
Input SAE	1.743	Car ls bad horse owner and handic apper Jon Lind o reinforced Santa An
Output SAE	1.431	Car ls bad horse owner and handic apper Jon Lind o reinforced Santa An
Jacobian	2.732×10^{-1}	Policy faculty members Ter ri Sab ol and Hann es Schw and t are among
Input SAE	2.084	Policy faculty members Ter ri Sab ol and Hann es Schw and t are among
Output SAE	1.030	Policy faculty members Ter ri Sab ol and Hann es Schw and t are among
Jacobian	2.731×10^{-1}	catch it . Y och was out at the intersection of Ott en and
Input SAE	2.490	catch it . Y och was out at the intersection of Ott en and
Output SAE	9.981×10^{-1}	catch it . Y och was out at the intersection of Ott en and

Table 4. The top 12 examples that produce the maximum absolute values of the Jacobian element with input SAE latent index 48028 and output latent index 64386. The Jacobian SAE pair was trained on layer 15 of Pythia-410m with an expansion factor of $R = 64$ and sparsity $k = 32$. The examples were collected over the first 10K records of the English subset of the C4 text dataset (Raffel et al., 2020), with a context length of 16 tokens. For each example, the first row shows the values of the Jacobian element, and the second and third show the corresponding activations of the input and output SAE latents. In this case, both SAE latents appear to weakly activate for tokens within proper nouns in German.

Category	Max. abs. value	Example tokens
Jacobian	2.530×10^{-1}	they are able to duplicate this to maneuver upon . Non Member \$ 1
Input SAE	1.659×10^1	they are able to duplicate this to maneuver upon . Non Member \$ 1
Output SAE	4.136	they are able to duplicate this to maneuver upon . Non Member \$ 1
Jacobian	2.530×10^{-1}	evaluates financial information for two segments : Se ismic and Non Se ismic .
Input SAE	1.655×10^1	evaluates financial information for two segments : Se ismic and Non Se ismic .
Output SAE	4.124	evaluates financial information for two segments : Se ismic and Non Se ismic .
Jacobian	2.508×10^{-1}	. Most patients go back to work the next day . Non surgical chin
Input SAE	1.835×10^1	. Most patients go back to work the next day . Non surgical chin
Output SAE	4.342	. Most patients go back to work the next day . Non surgical chin
Jacobian	2.507×10^{-1}	/ Non standard Fil ters " option so I guess I could use that
Input SAE	1.602×10^1	/ Non standard Fil ters " option so I guess I could use that
Output SAE	3.794	/ Non standard Fil ters " option so I guess I could use that
Jacobian	2.507×10^{-1}	out facial and neck wr inkles , the patient underwent Inf ini non invasive
Input SAE	1.775×10^1	out facial and neck wr inkles , the patient underwent Inf ini non invasive
Output SAE	4.175	out facial and neck wr inkles , the patient underwent Inf ini non invasive
Jacobian	2.507×10^{-1}	D err ata 2010 _ Q 3 Non conf idential Mark ed - up
Input SAE	1.686×10^1	D err ata 2010 _ Q 3 Non conf idential Mark ed - up
Output SAE	4.192	D err ata 2010 _ Q 3 Non conf idential Mark ed - up
Jacobian	2.502×10^{-1}	weeks , vigorous physical activity can be resumed . Non S urgical Chin
Input SAE	1.822×10^1	weeks , vigorous physical activity can be resumed . Non S urgical Chin
Output SAE	4.394	weeks , vigorous physical activity can be resumed . Non S urgical Chin
Jacobian	2.501×10^{-1}	smooth out facial wr inkles , the patient underwent Inf ini non invasive (
Input SAE	1.748×10^1	smooth out facial wr inkles , the patient underwent Inf ini non invasive (
Output SAE	4.139	smooth out facial wr inkles , the patient underwent Inf ini non invasive (
Jacobian	2.500×10^{-1}	those outcomes imply for the future . Non reactive – refers to an
Input SAE	1.765×10^1	those outcomes imply for the future . Non reactive – refers to an
Output SAE	4.052	those outcomes imply for the future . Non reactive – refers to an
Jacobian	2.493×10^{-1}	" fall protection for the most rigorous work environments . Non sl ip chest
Input SAE	1.830×10^1	" fall protection for the most rigorous work environments . Non sl ip chest
Output SAE	4.290	" fall protection for the most rigorous work environments . Non sl ip chest
Jacobian	2.491×10^{-1}	basis . Non profit is the only exception to these terms of agreement you
Input SAE	1.665×10^1	basis . Non profit is the only exception to these terms of agreement you
Output SAE	3.990	basis . Non profit is the only exception to these terms of agreement you
Jacobian	2.489×10^{-1}	OR GAN IC . NON G MO , C ERT IF IED K OS
Input SAE	1.474×10^1	OR GAN IC . NON G MO , C ERT IF IED K OS
Output SAE	3.587	OR GAN IC . NON G MO , C ERT IF IED K OS

Table 5. The top 12 examples that produce the maximum absolute values of the Jacobian element with input SAE latent index 26438 and output latent index 54734. The Jacobian SAE pair was trained on layer 15 of Pythia-410m with an expansion factor of $R = 64$ and sparsity $k = 32$. The examples were collected over the first 10K records of the English subset of the C4 text dataset (Raffel et al., 2020), with a context length of 16 tokens. For each example, the first row shows the values of the Jacobian element, and the second and third show the corresponding activations of the input and output SAE latents. In this case, both SAE latents appear to strongly activate for the pair of tokens ‘non-’ (in upper- or lowercase).

Jacobian Sparse Autoencoders: Sparsify Computations, Not Just Activations

Category	Max. abs. value	Example tokens
Jacobian	2.331×10^{-1}	s favourite chefs . The exciting event has not only been about fun and
Input SAE	5.784	s favourite chefs . The exciting event has not only been about fun and
Output SAE	2.349	s favourite chefs . The exciting event has not only been about fun and
Jacobian	2.313×10^{-1}	cup dec an ter brew ers . Special paper grade ass ures optimum extraction of
Input SAE	1.220	cup dec an ter brew ers . Special paper grade ass ures optimum extraction of
Output SAE	1.417	cup dec an ter brew ers . Special paper grade ass ures optimum extraction of
Jacobian	2.302×10^{-1}	working one - on - one with the pur vey ors of food .
Input SAE	1.184	working one - on - one with the pur vey ors of food .
Output SAE	3.366	working one - on - one with the pur vey ors of food .
Jacobian	2.292×10^{-1}	ns cater ing specifically to the Japanese tourist . For many Japanese visitors Bro ome
Input SAE	1.161	ns cater ing specifically to the Japanese tourist . For many Japanese visitors Bro ome
Output SAE	2.027	ns cater ing specifically to the Japanese tourist . For many Japanese visitors Bro ome
Jacobian	2.275×10^{-1}	's re pert ory production Creative Con vergence . In March , Peter Pan
Input SAE	1.527	's re pert ory production Creative Con vergence . In March , Peter Pan
Output SAE	8.890×10^{-1}	's re pert ory production Creative Con vergence . In March , Peter Pan
Jacobian	2.275×10^{-1}	Pe aks Brewing Company , beer offerings and specialty menu items . PU B 365
Input SAE	5.791	Pe aks Brewing Company , beer offerings and specialty menu items . PU B 365
Output SAE	2.536	Pe aks Brewing Company , beer offerings and specialty menu items . PU B 365
Jacobian	2.273×10^{-1}	um min ess from local chocol at ier Eclipse Chocolate ! Chocolate Un w
Input SAE	1.811	um min ess from local chocol at ier Eclipse Chocolate ! Chocolate Un w
Output SAE	1.769	um min ess from local chocol at ier Eclipse Chocolate ! Chocolate Un w
Jacobian	2.272×10^{-1}	food establishment to have a Cert ified Food Protection Manager (C FP M)
Input SAE	2.957	food establishment to have a Cert ified Food Protection Manager (C FP M)
Output SAE	3.219	food establishment to have a Cert ified Food Protection Manager (C FP M)
Jacobian	2.271×10^{-1}	and Steve from Si ren Craft Brew s Bar rel Project have team ed up
Input SAE	1.034	and Steve from Si ren Craft Brew s Bar rel Project have team ed up
Output SAE	1.831	and Steve from Si ren Craft Brew s Bar rel Project have team ed up
Jacobian	2.270×10^{-1}	first event came up unexpectedly , the Bridge and T unnel Brew ery was just
Input SAE	1.922	first event came up unexpectedly , the Bridge and T unnel Brew ery was just
Output SAE	1.807	first event came up unexpectedly , the Bridge and T unnel Brew ery was just
Jacobian	2.269×10^{-1}	in other colors , ordering in colors other than fl orescent green or orange WILL
Input SAE	1.327	in other colors , ordering in colors other than fl orescent green or orange WILL
Output SAE	1.055	in other colors , ordering in colors other than fl orescent green or orange WILL
Jacobian	2.269×10^{-1}	eating out or not buying a new BMW creates job cuts but not def lation
Input SAE	2.020	eating out or not buying a new BMW creates job cuts but not def lation
Output SAE	2.951	eating out or not buying a new BMW creates job cuts but not def lation

Table 6. The top 12 examples that produce the maximum absolute values of the Jacobian element with input SAE latent index 54846 and output latent index 30912. The Jacobian SAE pair was trained on layer 15 of Pythia-410m with an expansion factor of $R = 64$ and sparsity $k = 32$. The examples were collected over the first 10K records of the English subset of the C4 text dataset (Raffel et al., 2020), with a context length of 16 tokens. For each example, the first row shows the values of the Jacobian element, and the second and third show the corresponding activations of the input and output SAE latents. In this case, both SAE latents appear to activate for tokens or contexts relating to food service.